A New Framework and Software to Estimate Time-Varying Reproduction Numbers During Epidemics

Article *in* American Journal of Epidemiology · September 2013

DOI: 10.1093/aje/kwt133 · Source: PubMed

4 authors, including:

Anne Cori
Imperial College London
136 PUBLICATIONS **7,332** CITATIONS
SEE PROFILE

Neil Ferguson
Imperial College London
220 PUBLICATIONS **27,832** CITATIONS
SEE PROFILE

Christophe Fraser
Imperial College London
423 PUBLICATIONS **28,482** CITATIONS
SEE PROFILE

American Journal of Epidemiology Advance Access published September 15, 2013

American Journal of Epidemiology

DOI: 10.1093/aje/kwt133

Practice of Epidemiology

A New Framework and Software to Estimate Time-Varying Reproduction Numbers During Epidemics

Anne Cori*, Neil M. Ferguson, Christophe Fraser, and Simon Cauchemez

* Correspondence to Dr. Anne Cori, Department of Infectious Disease Epidemiology, MRC Centre for Outbreak Analysis and Modelling, Imperial College London, St Mary's Campus, Norfolk Place, London W2 1PG, United Kingdom (e-mail: a.cori@imperial.ac.uk).

Initially submitted November 26, 2012; accepted for publication May 23, 2013.

The quantification of transmissibility during epidemics is essential to designing and adjusting public health responses. Transmissibility can be measured by the reproduction number *R*, the average number of secondary cases caused by an infected individual. Several methods have been proposed to estimate *R* over the course of an epidemic; however, they are usually difficult to implement for people without a strong background in statistical modeling. Here, we present a ready-to-use tool for estimating *R* from incidence time series, which is implemented in popular software including Microsoft Excel (Microsoft Corporation, Redmond, Washington). This tool produces novel, statistically robust analytical estimates of *R* and incorporates uncertainty in the distribution of the serial interval (the time between the onset of symptoms in a primary case and the onset of symptoms in secondary cases). We applied the method to 5 historical outbreaks; the resulting estimates of *R* are consistent with those presented in the literature. This tool should help epidemiologists quantify temporal changes in the transmission intensity of future epidemics by using surveillance data.

incidence; influenza; measles; reproduction number; SARS; smallpox; software

Abbreviations: CI, credible interval; SARS, severe acute respiratory syndrome.

The reproduction number, *R*, is the average number of secondary cases of disease caused by a single infected individual over his or her infectious period. This statistic, which is time and situation specific, is commonly used to characterize pathogen transmissibility during an epidemic. The monitoring of *R* over time provides feedback on the effectiveness of interventions and on the need to intensify control efforts (1–4), given that the goal of control efforts is to reduce *R* below the threshold value of 1 and as close to 0 as possible, thus bringing an epidemic under control.

A wide range of methods have been proposed to estimate *R* from surveillance data (5–12). However, methods based on fitting mechanistic transmission models to incidence data are often difficult to generalize because of the context-specific assumptions often made (e.g., presence/absence of a latency period or size of the population studied). Recently, a simpler statistical approach was proposed, which addressed this issue. The Wallinga and Teunis method (13) is generic and requires only case incidence data and the distribution of the serial interval (the time between the onset of symptoms in a primary case and the onset of symptoms of secondary cases) to estimate *R* over the course of an epidemic. It is based on the probabilistic reconstruction of transmission trees and on counting the number of secondary cases per infected individual. The method estimates 1 value of *R* per time step of incidence (typically, per day).

However, the approach has several drawbacks. First, estimates are right censored, because the estimate of *R* at time *t* requires incidence data from times later than *t*. Approaches to correct for this issue have been developed (14).

When the data aggregation time step is small (e.g., daily data), estimates of *R* can vary considerably over short time periods, producing substantial negative autocorrelation. Other studies have developed methods to achieve smoother estimates, but the results can be sensitive to the selected time step or to smoothing parameters (15–18).

The implementation of these methods requires time and expertise, especially to produce confidence or credible intervals

for R. Hence, although there are many methods to quantify transmissibility during an epidemic, none currently comes as a ready-to-use tool for nonmodelers.

The aim of our study was to develop a generic and robust tool for estimating the time-varying reproduction number, similar in spirit to earlier methods, but implemented with ready-to-use software and without the drawbacks mentioned above. We provide Microsoft Excel (Microsoft Corporation, Redmond, Washington) and R software (R Foundation for Statistical Computing, Vienna, Austria) versions of this tool, and a user-friendly web interface will soon be available, as well. (The use of the letter R to denote both the reproduction number and the software package is coincidental).

After describing our approach, we apply it to data from selected historical outbreaks of pandemic influenza, severe acute respiratory syndrome (SARS), measles, and smallpox.

MATERIALS AND METHODS

A more detailed description of our methods can be found in the Web Appendices 1–13 available at http://aje.oxfordjournals.org/.

We assume that, once infected, individuals have an infectivity profile given by a probability distribution w_s, dependent on time since infection of the case, s, but independent of calendar time, t. For example, an individual will be most infectious at time s when w_s is the largest. The distribution w_s typically depends on individual biological factors such as pathogen shedding or symptom severity.

The instantaneous reproduction number (19), R_t, can be estimated by the ratio of the number of new infections generated at time step t, I_t, to the total infectiousness of infected individuals at time t, given by $\sum_{s=1}^{t} I_{t-s}w_s$, the sum of infection incidence up to time step $t-1$, weighted by the infectivity function w_s. R_t is the average number of secondary cases that each infected individual would infect if the conditions remained as they were at time t.

In practice, contact rates and transmissibility can change over time, particularly when control measures are initiated. This affects the number of secondary cases that a given individual infected at time step t will actually infect. The case reproduction number at time step t, R_t^c, takes into account those changes. It is the average number of secondary cases that a case infected at time step t will eventually infect (19). It is sometimes called the cohort reproduction number because it counts the average number of secondary transmissions caused by a cohort infected at time step t. However, estimation of R_t^c can be undertaken only in retrospect, once the secondary cases generated by cases infected at t have been infected. R_t^c is the quantity estimated in Wallinga and Teunis–type approaches (although the Wallinga and Teunis method considers cohorts of individuals with symptom onset at time t rather than infection at time t) (13).

The distinction between R_t^c and R_t is similar to the distinction between the actual life span of individuals born in 2013, which we can measure only retrospectively after all individuals have died (i.e., in a century), and life expectancy in 2013, estimated now by assuming that death rates in the future will be similar to those in 2013.

R_t is the only reproduction number easily estimated in real time. Moreover, effective control measures undertaken at time t are expected to result in a sudden decrease in R_t and a smoother decrease in R_t^c (19). Hence, assessing the efficiency of control measures is easier by using estimates of R_t. For these reasons, we focus on estimating the instantaneous reproduction number R_t in this article. (See Wallinga and Teunis (13), and Cauchemez et al. (14, 15) for methods used to estimate the case reproduction number).

Given the definition of R_t stated above, the incidence of cases at time step t is, on average, $\mathbf{E}[I_t] = R_t \sum_{s=1}^{t} I_{t-s}w_s$, where $\mathbf{E}[X]$ denotes the expectation of a random variable X, and I_{t-s} is the incidence at time step $t-s$ (19). Bayesian statistical inference based on this transmission model leads to a simple analytical expression of the posterior distribution of R_t if we assume a gamma prior distribution for R_t. This makes obtaining any desired characteristic of this posterior distribution (e.g., the median, the variance, or the 95% credible interval) straightforward (Web Appendix 1).

However, the resulting R_t estimates can be highly variable and hence difficult to interpret when the time step of data is small (20). We therefore calculate estimates over longer time windows, under the assumption that the instantaneous reproduction number is constant within that time window. At each time step t, we calculate the reproduction number over a time window of size τ ending at time t. These estimates, denoted $R_{t,\tau}$, quantify the average transmissibility over a time window of length τ ending at time t. They are expected to be less variable as the window size τ increases, because 2 successive time windows will then have increasing overlap. As τ increases, the estimates of $R_{t,\tau}$ will also be more precise. In fact, we show in Web Appendix 2 that the precision of these estimates depends directly on the number of incident cases in the time window $[t-\tau+1; t]$. This allows us to control the precision by adjusting the window size.

We also provide estimates of $R_{t,\tau}$ that take into account the uncertainty in the serial interval distribution parameters by integrating over a range of means and standard deviations of the serial interval (Web Appendix 4).

The estimation method presented above is developed for the ideal situation in which times of infection are known and the infectivity profile w_s may be approximated by the distribution of the generation time (i.e., time from the infection of a primary case to infection of the cases he/she generates) (19). However, times of infection are rarely observed, and the generation time distribution is therefore difficult to measure. On the other hand, the timing of onset of symptoms is usually known, and such data collected in closed settings where transmission can reliably be ascertained (e.g., households) can be used to estimate the distribution of the serial interval (time between onset of symptoms of a case and onset of symptoms of his/her secondary cases). Therefore, in practice, we apply our method to data consisting of daily counts of onset of symptoms where the infectivity profile w_s is approximated by the distribution of the serial interval.

For many diseases, including influenza (21), SARS (22), measles (23), and smallpox (24), it is expected that infectiousness starts only around the time of symptom onset. In such diseases, and when the infectiousness profile after symptoms is independent of the incubation period, the distributions

of the serial interval and the generation time are identical (Web Appendix 9), and our estimates are exact (albeit with t defined as the time of symptom onset of a primary case and a time lag in our estimates of R_t equal to the incubation period).

We provide a Microsoft Excel spreadsheet (available at http://tools.epidemiology.net/EpiEstim.xls) that implements the estimation method described above. Documentation on how to use the Microsoft Excel file is provided in Web Appendix 14. We have also developed an R package, EpiEstim, which can be downloaded at http://cran.r-project.org/web/packages/EpiEstim/index.html, in which both our method and the Wallinga and Teunis method (13) are implemented to facilitate comparison. We also developed a user-friendly web interface that will soon be available at http://shiny.epidemiology.net/EpiEstim.

RESULTS

To illustrate the insights that our method can provide, we applied it to 5 historical epidemics that varied in terms of transmissibility, serial interval, and population size. For each epidemic, we retrieved the epidemic curve, as well as the mean and standard deviation of the serial interval, from the literature (Table 1). The discrete distribution of the serial interval, w_s, was then obtained by assuming a gamma distribution (Web Appendix 11). For each day t of each epidemic, we estimated the reproduction number for the weekly window ending on that day ($R_{t,\tau=7}$, now denoted R for simplicity). The 5 epidemic curves, serial interval distributions, and R estimates are presented in Figure 1. Estimates are not shown from the very beginning of each epidemic because precise estimation is not possible in this period (Web Appendix 3). The estimated case reproduction numbers for those 5 epidemics are also shown in Figure 1 for comparison.

Measles in Hagelloch, Germany, 1861

R initially decreased from an initial median value of 4.3 (95% credible interval (CI): 2.0–8.2) in the middle of the third week to 3.0 (95% CI: 1.3–5.9) at the end of the same week, and then increased to 11.5 (95% CI: 8.3–15.3) in the middle of week 4, and finally decreased again until the end of the epidemic, falling below 1 at the beginning of week 7.

The increase in R from weeks 3 to 4 suggests increasing transmissibility. Previous studies have highlighted the importance of the structure (by classroom and household) of the contact network in this epidemic and have suggested the existence of early "superspreaders" (25). These characteristics could explain the increase in R. Interestingly, just after the first peak of incidence, R was still above 1, indicating that the epidemic was not yet over; and indeed, a second peak was still to come.

Pandemic influenza in Baltimore, Maryland, 1918

This epidemic curve was characterized by 2 days with unusually high incidence, on the 1st and the 15th of October 1918 (days 31 and 45). This might be related to a recollection bias, because the data were collected after the epidemic. Although we used a 1-week ($\tau = 7$) time window to calculate R, estimates still fluctuated. We found an initial median estimate of R of 1.4 (95% CI: 1.0–1.9) at the end of week 2. Estimates were then quite stable until R peaked at 2.4 (95% CI: 2.2–2.6) in the middle of week 5 (coincident with the second highest peak in incidence). Estimates then decreased, with R falling below 1 early in week 7, before the largest peak in incidence (though around that peak, R estimates just exceed 1 for a few days). At the very end of the epidemic, the credible intervals widen because of low case numbers.

Table 1. Description of the 5 Data Sets Analyzed, Corresponding to 5 Epidemics Between 1861 and 2009

First Author, Year (Reference No.)	Disease	Location	Year of Epidemic	Incidence of[a]	Mean (SD) Serial Interval, days	Reference for Mean (SD) Serial Interval
Groendyke, 2011 (37)	Measles	Hagelloch, Germany	1861	Onset of early symptoms	14.9 (3.9)	Derived from Groendyke et al. (37)[b]
White, 2008 (17); Fraser, 2011 (20); Frost, 1919 (38); Vynnycky, 2007 (39)	Pandemic influenza	Baltimore, Maryland	1918	Onset of symptoms	2.6 (1.5)	Ferguson et al. (40); Boelle et al. (41)
Fenner, 1988 (26); Gani, 2001 (42)	Smallpox	Kosovo	1972	Onset of symptoms	22.4 (6.1)	Derived from Riley and Ferguson (43)[b]
Cori, 2009 (16)	SARS	Hong Kong	2003	Onset of symptoms	8.4 (3.8)	Lipsitch et al. (44)
Cauchemez, 2011 (31)	Pandemic influenza	School in Pennsylvania	2009	Onset of acute respiratory illness among children attending the school	2.6 (1.5)	Ferguson et al. (40); Boelle et al. (41)

Abbreviations: SARS, severe acute respiratory syndrome; SD, standard deviation.

[a] Clinical characteristic considered to define the incidence. The incidence at time step t is the number of individuals showing this clinical characteristic at time step t.

[b] Estimates of the mean and standard deviation of the generation time for measles and smallpox were not available directly from the literature. Instead, we derived them indirectly from published estimates of the latency and infectious periods. Technical details about this derivation are described in Web Appendix 13.

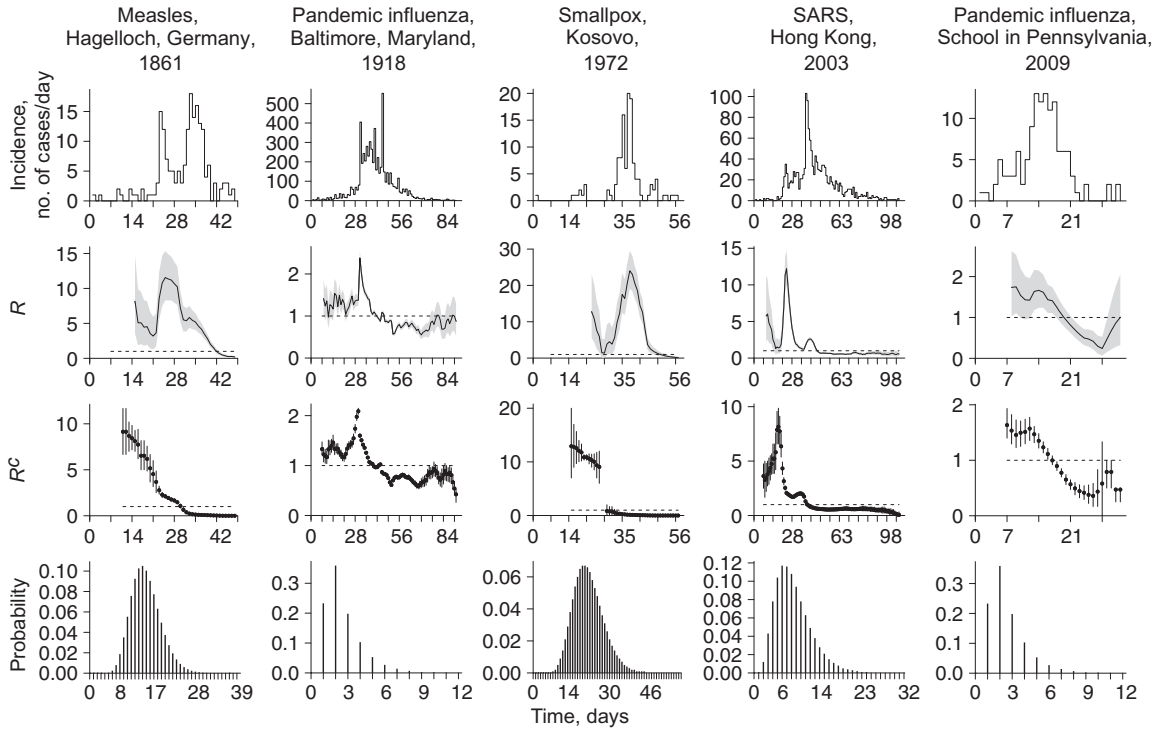

Figure 1. The first row shows daily epidemic curves (from left to right) for measles in Hagelloch, Germany, October 1861–January 1862; pandemic influenza in Baltimore, Maryland, September–November 1918; smallpox in Kosovo, February–April 1972; severe acute respiratory syndrome (SARS) in Hong Kong, February–June 2003; and pandemic influenza in a school in Pennsylvania, April–May 2009. The second row shows daily estimates of the instantaneous reproduction numbers R over sliding weekly windows; the black lines show the posterior medians and the grey zones show the 95% credible intervals; the horizontal dashed lines indicate the threshold value $R = 1$. The third row shows daily estimates of the case reproduction numbers R^c over sliding weekly windows; the black dots show the mean estimates, and the bars show the 95% confidence intervals; the horizontal dashed lines indicate the threshold value $R^c = 1$. The fourth row shows the serial interval distributions used for estimation of R and R^c.

Fraser et al. (20) found a similar temporal trend for R and attributed the decrease in R to social distancing measures that were undertaken around October 10 (day 40). This is consistent with our analysis (given that we were looking at R estimates over the past week) in which R fell below 1 on day 43.

Because the serial interval distribution for the 1918 pandemic is poorly documented, we explored a range of means and standard deviations for the serial interval and derived estimates of R by integrating over all these values (Web Appendix 4). The results are shown in Figure 2. The median estimated R in the presence of this uncertainty differed by 3% or less from the estimates obtained with a fixed serial interval distribution. However, the credible intervals were wider, reflecting the increased uncertainty.

We also examined the choice of the assumed time window width used to estimate R for this data set. Figure 3 shows daily estimates of R for 1-day, 1-week, 2-week, and 4-week windows, assuming a known serial interval distribution (as in Table 1). The estimates varied substantially according to the window size chosen. The 1-day window estimates were so variable that it was hard to derive any trend from them. As the window size grew, the median estimates were smoother, and the credible intervals were narrower, as expected. For 4-week windows, the upper credible interval was below 1 at the end of the epidemic. However, longer intervals delayed the time at which the median estimated R fell below 1. Overall, for this data set, a 1-week window represents a good compromise.

Smallpox in Kosovo, 1972

The analysis of the smallpox outbreak in Kosovo in 1972 illustrates the potentially long delay between the first case and the time when it is reasonable to start estimating R. Here, for a small epidemic with a long mean serial interval, that delay was as long as 4 weeks. We found that R increased from a median value of 3.4 (95% CI: 0.8–9.3) early in the fourth week to 23.9 (95% CI: 19.0–29.5) in the middle of week 6 and then decreased again until the end of the epidemic, falling below 1 only in the beginning of week 8.

The initial increase in R is consistent with a report that identified that transmission during the "second generation of cases" was unusually high, which the authors assumed to be "associated with inadequate protection from vaccination" (26). Estimates stayed above 1 until very late in the epidemic, indicating the limited success of control measures.

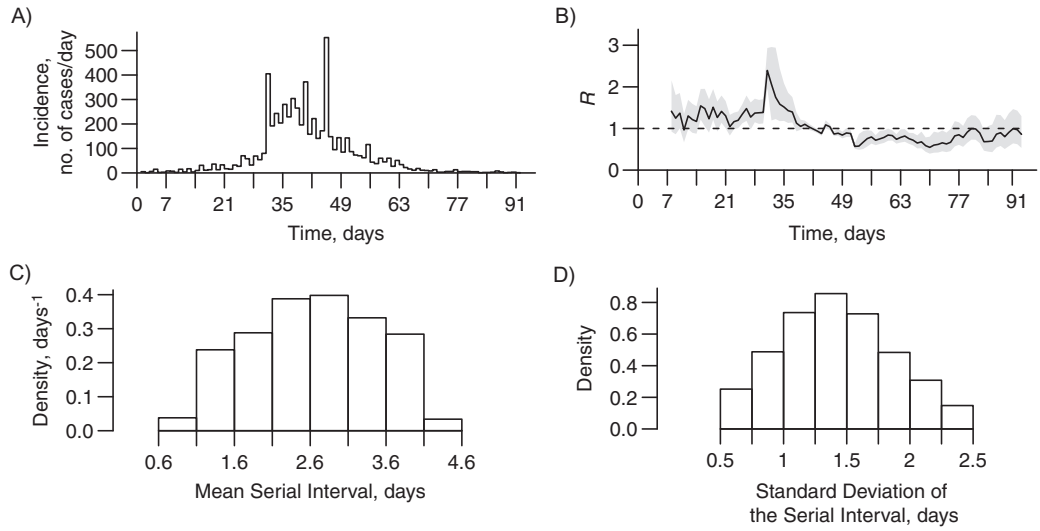

Figure 2. Estimated reproduction number for pandemic influenza in Baltimore, Maryland, September–November 1918. A) Daily epidemic curve; B) daily estimates of the reproduction number R over sliding weekly windows (the black line shows the posterior medians and the grey zones show the 95% credible intervals; the horizontal dashed line indicates the threshold value $R = 1$); C) histogram of the mean serial intervals explored; and D) histogram of the standard deviations of the serial interval explored.

Vaccination, which started on March 16 (day 31) was slow (95% coverage was achieved only by the end of April, around day 70) and sometimes ineffective (26).

SARS in Hong Kong, 2003

For the SARS outbreak in Hong Kong in 2003, we find 2 successive peaks in R. The first occurred in the middle of week 3 with a median estimate of 12.2 (95% CI: 10.0–14.7), and the second occurred at the end of week 6 with a median estimate of 2.6 (95% CI: 2.4–2.9). R then fell below 1 by the end of week 7.

These 2 peaks coincide with the occurrence of known superspreading events, the first occurring in weeks 3 and 4, and the second occurring between weeks 5 and 6 (16, 27, 28). It is notable that R falls below 1 very quickly after the epidemic peak, while incidence is still quite high. Similar trends were found in previous analyses of this epidemic (13, 14).

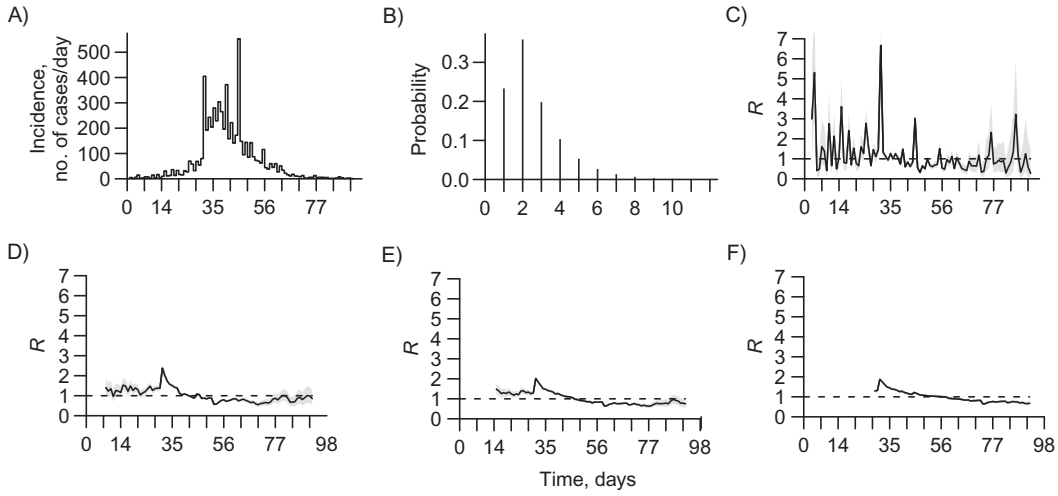

Figure 3. Estimated reproduction number for pandemic influenza in Baltimore, Maryland, September–November 1918, with several time windows. A) Daily epidemic curve; B) serial interval distribution; C–F) daily estimates of the reproduction numbers R over 1-day windows; C), over sliding weekly windows; D), over sliding 2-week windows; E) and over sliding 4-week windows; F) black lines show the posterior medians, and grey zones show the 95% credible intervals; the horizontal dashed lines indicate the threshold value $R = 1$.

Pandemic influenza in a school in Pennsylvania, 2009

We estimated that R was relatively constant over the whole second week of the epidemic, with a median around 1.7 (early in the week, 95% CI: 1.0–2.6; late in the week, 95% CI: 1.2–2.2). R then decreased, falling below 1 early in week 4. This could reflect the impact of control measures or could be due to the depletion of susceptibles in the school population. In the last days of the epidemic, 2 new cases appeared, probably as a result of reintroduction of infection from outside the school, resulting in estimates of R increasing again from a minimum value of 0.2 (95% CI: 0.1–0.5) to 0.9 (95% CI: 0.3–2.0).

Comparison between instantaneous reproduction number R and case reproduction number R^c

Figure 1 shows the instantaneous (R) and case (R^c) reproduction numbers estimated for the 5 epidemics. R^c was estimated by using the Wallinga and Teunis method (13), but on weekly windows (Web Appendix 5).

The estimates of R^c on weekly windows are smoother than the estimates of R on weekly windows. Moreover, they are ahead of the estimates of R by a mean serial interval. When the serial interval is short (e.g., for influenza or SARS), this delay is small, and the smoothing effect is not very strong. However, when the serial interval is long (e.g., for measles or smallpox), both effects are more dramatic, and the curves have very different interpretations. For the measles outbreak in Hallegoch, Germany, the highest estimate of R^c is early in the epidemic, on the week ending on day 11, which reflects high transmissibility 2 weeks later (i.e., on the week ending on day 25), coinciding exactly with the peak in the estimated R. This means that the high transmissibility around day 25 is due to cases who have shown symptoms, on average, 2 weeks earlier. Similarly, for the smallpox epidemic in Kosovo, the peak in R^c is on the week ending on day 15, and the peak in R is on the week ending on day 38 (i.e., 23 days later), which is the mean serial interval we have assumed. Transmissibility, measured by the instantaneous reproduction number, was very high during the second generation of cases, around day 38, but this was caused by the first generation of cases, who had symptoms around day 15.

DISCUSSION

We have developed a simple and generic method to estimate time-varying instantaneous reproduction numbers from incidence time series. A simulation study presented in Web Appendix 6 shows that our method is able to detect changes in the reproduction number, for instance, following a control measure. We applied this method to analyze the time course of transmissibility for 5 historical outbreaks. Our estimates of the instantaneous reproduction number are consistent with estimates of the case reproduction number despite considerable differences in interpretation. Our analyses are also in agreement with previously published results obtained with generally more complicated and less general methods.

For instance, although our estimates of the reproduction number for the 1918 influenza pandemic in Baltimore, Maryland, are similar to the maximum likelihood estimates obtained by Fraser et al. (20), it is much easier to produce credible intervals with our method than to produce confidence intervals with the previously used maximum likelihood estimates approach. Our method is also easier to implement and more flexible than the parametric estimation used by White and Pagano (17) on the same data set.

Similarly, for the 2003 SARS epidemic in Hong Kong, Wallinga and Teunis (13), as well as Cauchemez et al. (14), found temporal trends for the case reproduction number similar to our estimates of the instantaneous reproduction number but with lower peak values. The case reproduction number (which is the quantity derived in those studies) is estimated over a generation of infection (i.e., over 8.4 days on average for SARS). When the instantaneous reproduction number is estimated on time windows shorter than the average generation time (which is the case for our weekly windows), we expect the case reproduction to be smoother than the instantaneous reproduction number, which could explain why we find higher peaks. Again, it is more straightforward to produce credible intervals with our method than it is with those approaches.

Robust estimation of R provides important insights into temporal changes in transmission during an epidemic. However, interpreting the temporal trends is not always straightforward. Changes in R can be due to changes in underlying transmissibility (e.g., due to seasonality), changes in contact patterns in the population affected, the impact of control measures, or the depletion of the size of the susceptible population. For instance, we found that R decreased very early during the SARS epidemic in Hong Kong. However, because many control measures were put in place at different times during the SARS epidemic (29, 30), it is difficult to relate the decrease seen directly to a specific control measure from this analysis alone.

Likewise, we estimated that, for the outbreak of 2009 pandemic influenza in a school in Pennsylvania, there was again an early decrease in R. But just estimating R does not allow us to determine whether this reflects a true reduction in transmissibility, possibly due to the school closure between May 14–20 (days 17–23) or the depletion of susceptibles. By using a more complex analysis, Cauchemez et al. (31) showed that the second of these explanations was more likely.

The method developed here relies on knowledge of the serial interval distribution but is able to directly incorporate uncertainty in serial interval distribution estimates**.** Allowing the mean and variance of the serial interval distribution to vary round average values affects median R estimates to a limited extent but increases the credible intervals around those estimates.

The estimates of R obtained with our method are quite sensitive to the size of the sliding window over which the estimates are calculated. Small windows can lead to highly variable estimates with wide credible intervals, whereas longer windows lead to smoothed estimates with narrower credible intervals. In Web Appendix 2, we discuss an interesting result on the minimum number of cases that need to be included in a time window to achieve a given precision in the estimate of R. Because the beginning of an epidemic has few incident cases, we used this result to provide guidance on when it is reasonable to start estimating R.

Finally, our method makes several assumptions that would benefit from reiteration. First, we applied our method to time series of onset of symptoms, and we used the serial interval

distribution as an approximation for the infectivity profile w_s. We showed in Web Appendix 12 that for diseases for which infectiousness starts only at the time of symptom onset, with an infectiousness profile after symptom onset independent of the incubation period, this leads to exact, but time-lagged, estimates of the reproduction number. Although for many diseases, including those studied here (21–24), this assumption is sensible, it does not hold for pathogens such as human immunodeficiency virus, for which infectiousness precedes symptoms (32).

In such cases, and if data on the incubation period (delay between infection and symptom onset) are available, a possible strategy would be to use the incubation period distribution to back-calculate the incidence of infections from the incidence of symptoms and then apply our method to estimate the reproduction number from those inferred data (19). However, this approach may lead to oversmoothed incidence time series compared with the true infection incidence (19).

Second, we assumed that all cases were detected. We showed in a simulation study that this should not dramatically affect estimates as long as the proportion of asymptomatic cases and the reporting rate are constant through time (Web Appendix 8). As an example, an early precursor of the method applied here was used to analyze time series of polio disease incidence, in which approximately 1 in 200 infections was symptomatic (33). In some situations, the reporting rate is likely to change over the course of an epidemic, for instance, as a result of improved case ascertainment or case definitions or changes in health care–seeking behavior over time. If data on reporting are available, it is possible to extend our method to take variable reporting rates into account (6).

We assumed that there were no imported cases, so that each incident case could be attributed to a previous case in the incidence time series. However, if imported cases were identified as such, our method could easily be adapted to account for them, as was done in previous studies by using other estimation methods (12, 34–36).

Finally, we assumed that the serial interval distribution was constant throughout the epidemic. However, if there were independent data (e.g., from contact tracing studies) suggesting evidence of changes in the serial interval distribution, our method could be applied with different serial interval distributions for different time periods of the epidemic.

Despite these assumptions, we feel the simplicity of the method we have presented here outweighs the limitations highlighted above. We hope our method will be adopted by epidemiologists and public health organizations. This will be facilitated by the R package and, more importantly, the simple Microsoft Excel tool and the web interface we have developed and released with this paper. These software programs should allow rapid analysis of incidence time series of any infectious disease within the scope described above and should be valuable tools for future outbreak investigations.

ACKNOWLEDGMENTS

Author affiliation: Department of Infectious Disease Epidemiology, MRC Centre for Outbreak Analysis and Modelling, Imperial College London, London, United Kingdom (Anne Cori, Neil M. Ferguson, Christophe Fraser, Simon Cauchemez).

This work was supported by the United Kingdom Medical Research Council methodology project G0800596, the FP7 European Management Platform for Emerging and Re-emerging Infectious Disease Entities project, and the National Institute of General Medical Sciences Models of Infectious Disease Agent Study program for support. S.C. was supported by the Research Council United Kingdom. C.F. holds a fellowship supported by the Royal Society.

We thank Dr. Thibaut Jombart for his help in developing the R package EpiEstim, and Dr. David Aanensen for his help in setting up the web interface.

Professor Christophe Fraser and Dr. Simon Cauchemez contributed equally to this work.

Conflict of interest: none declared.

REFERENCES

1. Anderson R, May R. *Infectious Diseases of Humans: Dynamics and Control*. Oxford, United Kingdom: Oxford University Press; 1991.
2. Ferguson NM, Cummings DA, Fraser C, et al. Strategies for mitigating an influenza pandemic. *Nature*. 2006;442(7101):448–452.
3. Fraser C, Riley S, Anderson RM, et al. Factors that make an infectious disease outbreak controllable. *Proc Natl Acad Sci U S A*. 2004;101(16):6146–6151.
4. Anderson RM, May RM. Directly transmitted infectious diseases: control by vaccination. *Science*. 1982;215(4536):1053–1060.
5. Riley S, Fraser C, Donnelly CA, et al. Transmission dynamics of the etiological agent of SARS in Hong Kong: impact of public health interventions. *Science*. 2003;300(5627):1961–1966.
6. Fraser C, Donnelly CA, Cauchemez S, et al. Pandemic potential of a strain of influenza A (H1N1): early findings. *Science*. 2009;324(5934):1557–1561.
7. Ferguson NM, Donnelly CA, Anderson RM. Transmission intensity and impact of control policies on the foot and mouth epidemic in Great Britain. *Nature*. 2001;413(6855):542–548.
8. Amundsen EJ, Stigum H, Rottingen JA, et al. Definition and estimation of an actual reproduction number describing past infectious disease transmission: application to HIV epidemics among homosexual men in Denmark, Norway and Sweden. *Epidemiol Infect*. 2004;132(6):1139–1149.
9. Bettencourt LM, Ribeiro RM. Real time Bayesian estimation of the epidemic potential of emerging infectious diseases. *PLoS One*. 2008;3(5):e2185.
10. Cintron-Arias A, Castillo-Chavez C, Bettencourt LM, et al. The estimation of the effective reproductive number from disease outbreak data. *Math Biosci Eng*. 2009;6(2):261–282.
11. Howard SC, Donnelly CA. Estimation of a time-varying force of infection and basic reproduction number with application to an outbreak of classical swine fever. *J Epidemiol Biostat*. 2000;5(3):161–168.
12. Kelly HA, Mercer GN, Fielding JE, et al. Pandemic (H1N1) 2009 influenza community transmission was established in one Australian state when the virus was first identified in North America. *PLoS One*. 2010;5(6):e11341.

13. Wallinga J, Teunis P. Different epidemic curves for severe acute respiratory syndrome reveal similar impacts of control measures. *Am J Epidemiol*. 2004;160(6):509–516.
14. Cauchemez S, Boelle PY, Donnelly CA, et al. Real-time estimates in early detection of SARS. *Emerg Infect Dis*. 2006;12(1):110–113.
15. Cauchemez S, Boelle PY, Thomas G, et al. Estimating in real time the efficacy of measures to control emerging communicable diseases. *Am J Epidemiol*. 2006;164(6): 591–597.
16. Cori A, Boelle PY, Thomas G, et al. Temporal variability and social heterogeneity in disease transmission: the case of SARS in Hong Kong. *PLoS Comput Biol*. 2009;5(8):e1000471.
17. White LF, Pagano M. Transmissibility of the influenza virus in the 1918 pandemic. *PLoS One*. 2008;3(1):e1498.
18. Hens N, Van Ranst M, Aerts M, et al. Estimating the effective reproduction number for pandemic influenza from notification data made publicly available in real time: a multi-country analysis for influenza A/H1N1v 2009. *Vaccine*. 2011;29(5): 896–904.
19. Fraser C. Estimating individual and household reproduction numbers in an emerging epidemic. *PLoS One*. 2007;2(1):e758.
20. Fraser C, Cummings DA, Klinkenberg D, et al. Influenza transmission in households during the 1918 pandemic. *Am J Epidemiol*. 2011;174(5):505–514.
21. Lau LL, Cowling BJ, Fang VJ, et al. Viral shedding and clinical illness in naturally acquired influenza virus infections. *J Infect Dis*. 2010;201(10):1509–1516.
22. Peiris JS, Chu CM, Cheng VC, et al. Clinical progression and viral load in a community outbreak of coronavirus-associated SARS pneumonia: a prospective study. *Lancet*. 2003; 361(9371):1767–1772.
23. Simpson REH. Infectiousness of communicable diseases in the household (measles, chickenpox, and mumps). *Lancet*. 1952;2(6734):549–554.
24. Eichner M, Dietz K. Transmission potential of smallpox: estimates based on detailed data from an outbreak. *Am J Epidemiol*. 2003;158(2):110–117.
25. Groendyke C, Welch D, Hunter DR. *A Network-based Analysis of the 1861 Hagelloch Measles Data*. University Park, PA: Department of Statistics, Pennsylvania State University; 2011.
26. Fenner F, Henderson DA, Arita I, et al. *Smallpox and its Eradication*. Geneva, Switzerland: World Health Organization; 1988.
27. Lee N, Hui D, Wu A, et al. A major outbreak of severe acute respiratory syndrome in Hong Kong. *N Engl J Med*. 2003; 348(20):1986–1994.
28. Leung GM, Hedley AJ, Ho LM, et al. The epidemiology of severe acute respiratory syndrome in the 2003 Hong Kong epidemic: an analysis of all 1755 patients. *Ann Intern Med*. 2004;141(9):662–673.
29. SARS Expert Committee of HKSAR Government. Chronology of the SARS epidemic in Hong Kong. 2003. Hong Kong: SARS Expert Committee. (http://www.sars-expertcom.gov.hk/english/reports/reports/files/e_app3.pdf). (Accessed May 3, 2013).
30. World Health Organization. SARS: chronology of a serial killer. 2003. Geneva, Switzerland: World Health Organization. (http://www.who.int/csr/don/2003_07_04/en/print.html). (Accessed May 3, 2013).
31. Cauchemez S, Bhattarai A, Marchbanks TL, et al. Role of social networks in shaping disease transmission during a community outbreak of 2009 H1N1 pandemic influenza. *Proc Natl Acad Sci U S A*. 2011;108(7):2825–2830.
32. Babiker A, Darby S, De Angelis D, et al. Time from HIV-1 seroconversion to AIDS and death before widespread use of highly-active antiretroviral therapy: a collaborative re-analysis. *Lancet*. 2000;355(9210):1131–1137.
33. Grassly NC, Fraser C, Wenger J, et al. New strategies for the elimination of polio from India. *Science*. 2006;314(5802): 1150–1153.
34. Cowling BJ, Lau MS, Ho LM, et al. The effective reproduction number of pandemic influenza: prospective estimation. *Epidemiology*. 2010;21(6):842–846.
35. Nishiura H, Roberts MG. "Estimation of the reproduction number for 2009 pandemic influenza A(H1N1) in the presence of imported cases" [letter]. *Eurosurveillance*. 2010;15(29): 19–20.
36. Paine S, Mercer GN, Kelly PM, et al. Transmissibility of 2009 pandemic influenza A(H1N1) in New Zealand: effective reproduction number and influence of age, ethnicity and importations. *Eurosurveillance*. 2010;15(24): 9–17.
37. Groendyke C, Welch D, Hunter DR. Bayesian inference for contact networks given epidemic data. *Scand J Stat*. 2011; 38(3):600–616.
38. Frost WH, Sydenstricker E. Influenza in Maryland: preliminary statistics of certain localities. *Public Health Rep*. 1919;34(11):491–504.
39. Vynnycky E, Trindall A, Mangtani P. Estimates of the reproduction numbers of Spanish influenza using morbidity data. *Int J Epidemiol*. 2007;36(4):881–889.
40. Ferguson NM, Cummings DA, Cauchemez S, et al. Strategies for containing an emerging influenza pandemic in Southeast Asia. *Nature*. 2005;437(7056):209–214.
41. Boelle PY, Ansart S, Cori A, et al. Transmission parameters of the A/H1N1 (2009) influenza virus pandemic: a review. *Influenza Other Respi Viruses*. 2011;5(5):306–316.
42. Gani R, Leach S. Transmission potential of smallpox in contemporary populations. *Nature*. 2001;414(6865): 748–751.
43. Riley S, Ferguson NM. Smallpox transmission and control: spatial dynamics in Great Britain. *Proc Natl Acad Sci U S A*. 2006;103(33):12637–12642.
44. Lipsitch M, Cohen T, Cooper B, et al. Transmission dynamics and control of severe acute respiratory syndrome. *Science*. 2003;300(5627):1966–1970.

A new framework and software to estimate time-varying reproduction numbers during epidemics: web material

Contents

Web Appendix 1. Estimation of the instantaneous reproduction number

Following Fraser (1), we assume that the distribution of infectiousness through time after infection is independent of calendar time. We model transmission with a Poisson process, so that the rate at which someone infected in time step $t-s$ generates new infections in time step *t*, is equal to $R_t w_s$, where R_t is the instantaneous reproduction number at time t and w_s a probability distribution (hence summing to 1) describing the average infectiousness profile after infection. Therefore the incidence at time t is Poisson distributed with mean $R_t \sum_{s=1}^{t} I_{t-s} w_s$, and the likelihood of the incidence I_t given the reproduction number R_t, conditional on the previous incidences $I_0,\ldots I_{t-1}$, is:

$$P\left(I_t \mid I_0,\ldots,I_{t-1},w,R_t\right)=\frac{\left(R_t\Lambda_t\right)^{I_t} e^{-R_t\Lambda_t}}{I_t!}$$

with $\Lambda_t = \sum_{s=1}^{t} I_{t-s} w_s$.

Now, if transmissibility is assumed constant over a time period $\left[t-\tau+1;t\right]$, measured by the reproduction number noted $R_{t,\tau}$, the likelihood of the incidence during this time period, $I_{t-\tau+1},\ldots,I_t$ given the reproduction number $R_{t,\tau}$, conditional on the previous incidences $I_0,\ldots I_{t-\tau}$, is:

$$P\left(I_{t-\tau+1},\ldots,I_t \mid I_0,\ldots,I_{t-\tau},w,R_{t,\tau}\right)=\prod_{s=t-\tau+1}^{t}\frac{\left(R_{t,\tau}\Lambda_s\right)^{I_s} e^{-R_{t,\tau}\Lambda_s}}{I_s!}.$$

Using a Bayesian framework with a Gamma distributed prior with parameters (a,b) for $R_{t,\tau}$, the posterior joint distribution of $R_{t,\tau}$ is

$$\begin{aligned}P\left(I_{t-\tau+1},\ldots,I_t,R_{t,\tau} \mid I_0,\ldots,I_{t-\tau},w\right) &= P\left(I_{t-\tau+1},\ldots,I_t \mid I_0,\ldots,I_{t-\tau},w,R_{t,\tau}\right)P\left(R_{t,\tau}\right)\\ &= \left(\prod_{s=t-\tau+1}^{t}\frac{\left(R_{t,\tau}\Lambda_s\right)^{I_s} e^{-R_{t,\tau}\Lambda_s}}{I_s!}\right)\left(\frac{R_{t,\tau}^{a-1} e^{-R_{t,\tau}/b}}{\Gamma(a)b^a}\right)\\ &= R_{t,\tau}^{a+\sum_{s=t-\tau+1}^{t} I_s-1} e^{-R_{t,\tau}\left(\sum_{s=t-\tau+1}^{t}\Lambda_s+\frac{1}{b}\right)}\prod_{s=t-\tau+1}^{t}\frac{\Lambda_s^{I_s}}{I_s!}\frac{1}{\Gamma(a)b^a}\end{aligned}$$

Which is proportional to:

$$R_{t,\tau}^{\,a+\sum_{s=t-\tau+1}^{t} I_s - 1} e^{-R_{t,\tau}\left(\sum_{s=t-\tau+1}^{t} \Lambda_s + \frac{1}{b}\right)} \prod_{s=t-\tau+1}^{t} \frac{\Lambda_s^{\,I_s}}{I_s!}.$$

Therefore, the posterior distribution of $R_{t,\tau}$ is a Gamma distribution with parameters $\left(a+\sum_{s=t-\tau+1}^{t} I_s, \frac{1}{\frac{1}{b}+\sum_{s=t-\tau+1}^{t}\Lambda_s}\right)$. In particular, the posterior mean of $R_{t,\tau}$ is $\frac{a+\sum_{s=t-\tau+1}^{t} I_s}{\frac{1}{b}+\sum_{s=t-\tau+1}^{t}\Lambda_s}$, and the posterior coefficient of variation (CV, standard deviation divided by mean) of $R_{t,\tau}$ is $\frac{1}{\sqrt{a+\sum_{s=t-\tau+1}^{t} I_s}}$.

The results shown in the main text were obtained using a Gamma prior distribution with mean 5 and standard deviation 5 (therefore $a=1, b=5$) for each $R_{t,\tau}$.

Web Appendix 2. Choice of time window

The estimates of R are expected to depend on the choice of the time window size τ. Small values of τ lead to more rapid detection of changes in transmission but also more statistical noise; large values lead to more smoothing, and reductions in statistical noise. So how to choose the appropriate time window?

Having an analytical formulation of the posterior distribution of R allowed us to link the posterior CV to the number of incident cases in the time window considered (see section Web Appendix 1). Imposing a posterior CV smaller than a predetermined threshold value $CV_{threshold}$ leads to $\sum_{s=t-\tau+1}^{t} I_s \geq \frac{1}{CV_{threshold}^{\,2}} - a$. This gives a minimum bound to the number of incident cases in the time window considered. Note that this result is independent on the infectiousness profile.

Web Table 1 presents the minimum number of incident cases in each time window corresponding to different choices of prior CV and aimed posterior CV. This result can provide guidance on the time windows to consider.

Web Table 1: Minimum number of incident cases in each time window as a function of the aimed posterior coefficient of variation (CV) for different choices of the prior coefficient of variation.

Prior CV	Aimed posterior CV									
	1	**0.9**	**0.8**	**0.7**	**0.6**	**0.5**	**0.4**	**0.3**	**0.2**	**0.1**
1	0	1	1	2	2	3	6	11	24	99
2	1	1	2	2	3	4	6	11	25	100
5	1	2	2	3	3	4	7	12	25	100
10	1	2	2	3	3	4	7	12	25	100
10000	1	2	2	3	3	4	7	12	25	100

Web Appendix 3. When can we start estimating *R*?

For real-time estimates of R to be useful, we need to start computing them early during an epidemic. However, estimating R too early in the epidemic might not be possible, at least if a certain precision in the estimates is desired, for several reasons.

First, the estimate of R over a chosen time window can only be obtained at the end of that window, since it requires the observation of incident cases over the whole window.

Moreover, we saw in section Web Appendix 2 that the precision of the estimate is higher for a higher number of incident cases. To get a posterior CV of 0.3 for example (which is the aimed CV we used to get the results presented in the main text), the time window considered must comprise at least 11 incident cases (see Web Table 1). We therefore advise starting estimating R only after 12 (the initial case + 11) cases have been observed at total. Anyway, there is little chance that an epidemic in its very early stage, with <12 cases, would be detected, unless the symptoms are extremely severe.

Finally, the infectiousness profile should also provide guidance on when to start estimation. Indeed, estimating R before at least one generation of cases has been observed is difficult. For example, in the extreme case where generations are discrete, all cases in the second generation are infected at the same time *t* after the index case: it is therefore impossible to estimate R before that time *t*. Moreover, early in an outbreak, a substantial fraction of incident cases may be imported, which we do not account for in this study. Waiting until at least one average serial interval has passed should reduce the associated bias in the early estimates of R.

Overall, we suggest starting estimating R once those three criteria are fulfilled: at least after τ, at least after one mean serial interval, and when at least 12 cases have been observed since the beginning of the epidemic.

Web Appendix 4. Uncertainty in the infectiousness profile

Estimates of the reproduction number are highly dependent on the choice of the infectiousness profile w_s. This can be approximated by the distribution of the generation time (i.e. time from the infection of a primary case to infection of the cases he/she generates) (1). However, times of infection are rarely observed and the generation time distribution is therefore difficult to measure. On the other hand, the timing of symptoms onset is usually known and such data collected in closed settings where transmission can reliably be ascertained (e.g. households) can be used to estimate the distribution of the serial interval (time between symptoms onset of a case and symptoms onset of his/her secondary cases). Therefore, in practice, we apply our method on data consisting of daily counts of symptoms onset and where the infectivity profile w_s is approximated by the distribution of the serial interval. However, this distribution can be poorly documented, especially early in the epidemic. Here, we provide a method to explicitly take into account the uncertainty in the serial interval distribution. To do so, we assume that the serial interval is Gamma distributed, and we allow its mean μ_{SI} and standard deviation (sd) σ_{SI} to vary according to truncated normal distributions. We sample $n_{SI} = 1000$ pairs of mean and

sd: $(\mu_{SI},\sigma_{SI})^{(1)},\mathrm{K},(\mu_{SI},\sigma_{SI})^{(n_{SI})}$, by first sampling $\mu_{SI}{}^{(k)}$, and then sampling $\sigma_{SI}{}^{(k)}$ with the constraint that $\sigma_{SI}{}^{(k)} < \mu_{SI}{}^{(k)}$. This constraint ensures that the Gamma probability density function of the serial interval is null at $t=0$. For each pair $(\mu_{SI},\sigma_{SI})^{(k)}$, we then sample, for each sliding window of length τ, $n=1000$ realizations $R^{(k,1)},\ldots,R^{(k,n)}$ of R in its posterior distribution, conditional on $(\mu_{SI},\sigma_{SI})^{(k)}$, forming at total a sample of size $n\times n_{SI}=1,000,000$ of the joint posterior distribution of R.

We illustrated this method on the 1918 pandemic flu in Baltimore (see main text for the results), for which we used an average mean serial interval of 2.6 days (sd 1.5, min 1, max 4.2), and an average standard deviation of 1.5 days (sd 0.5, min 0.5, max 2.5).

Web Appendix 5. Estimation of the case reproduction number

In order to compare the our approach with the WT approach, we also estimated the case reproduction number $R^{c}_{t,\tau}$ using the Wallinga and Teunis (WT) method for the five dataset analysed in the main text as well as for the simulation study (see below). We estimated $R^{c}_{t,\tau}$, the average number of secondary cases infected by individuals with symptoms onset occurring during the time period $[t-\tau+1;t]$ (2). As in WT, we estimated the mean case reproduction number of individual *j* as: $R^{c}_{ind\ j}=\sum_{i}\frac{w_{t_i-t_j}}{\sum_{k,k\neq i}w_{t_i-t_k}}$, where t_i is the time of symptoms onset of individual *i* (2). The mean estimated case reproduction number over the time window $[t-\tau+1;t]$ was then estimated by averaging the individual case reproduction number over all those with symptoms onset in the considered time window: $R^{c}_{t,\tau}=\frac{\sum_{j,t-\tau+1\leq t_j\leq t}R^{c}_{ind\ j}}{\sum_{j,t-\tau+1\leq t_j\leq t}1}$. The confidence intervals were obtained by reconstructing a panel of possible infection trees using multinomial allocation of infectors. All the results presented here were obtained with 100 reconstructed trees. Note that no estimates are available for weeks with no incident cases.

For the simulation study, we derived the theoretical case reproduction number from the instantaneous reproduction number using the following formula: $R^{c}_{t}=\sum_{s=0}^{+\infty}R_{t+s}w_s$ (1).

Web Appendix 6. Simulation study

In order to assess the ability of our method to quantify transmissibility in several epidemic scenarios, we designed a simulation study based on two scenarios:

- constant instantaneous reproduction number $R = 2.5$,
- constant *R* before ($R = 2.5$) and after ($R = 0.7$) a certain date, illustrating the effect of a control measure such as school closure.

For each scenario, we simulated 100 epidemics, starting with 10 index cases. We used a SARS like serial interval distribution, with mean 8.4 days and standard deviation 3.8 days. We assumed a simple scenario with constant incubation period, so that the incidence of symptomatic cases is exactly the incidence of infections, but shifted in time. For each day $t \geq 2$, the number of incident cases I_t was drawn from a Poisson distribution with mean $R_t \sum_{s=1}^{t} I_{t-s} w_s$, where w_s is the discrete serial interval distribution. The epidemics were run for $T = 50$ days, with the intervention in scenario 2 occurring on day $T_e = 15$. For each simulated epidemic, we then reestimated, using our method, the instantaneous reproduction number $R_{t,\tau}$.

In order to compare the two approaches, we also estimated the case reproduction number $R^c_{t,\tau}$ using the Wallinga and Teunis (WT) method (see previous section) (2).

The simulated epidemics are shown in Web Figure 1 and the corresponding estimated reproduction numbers shown in Web Figures 2 and 3.

Our method allows reestimating the instantaneous reproduction number used for simulation. Unlike the WT method, it does not suffer of the right censoring, i.e. estimates of the reproduction number at the very end of the time series accurately reflect the transmissibility at that time point and do not artefactually decrease to zero due to lack of observation of secondary cases in the future (see Web Figure 2). However it's worth mentioning that methods inspired from the WT method have been developed to overcome this issue (3).

The case reproduction number $R^c_{t,1}$ on a day t reflects transmissibility over a time period starting on day t and lasting for one serial interval, whereas the instantaneous reproduction number $R_{t,1}$ on day t reflects transmissibility on a single day. Therefore $R^c_{t,1}$ is smoother than $R_{t,1}$ (1). Similarly for any given window size τ, the instantaneous *R* over that window estimated with our method is more variable from one time window to the next than the corresponding case R^c (see Web Figure 2).

Interestingly, our method allows detecting changes in the instantaneous reproduction number, for instance a decrease in transmissibility following a control measure. These features are more difficult to detect when estimating R^c because it is not an instantaneous measure of transmissibility, and therefore its variations are much smoother over time (see Web Figure 3).

Using larger time windows allows getting smoother estimates of *R*, which leads to smoother but delayed curves and lowers the ability to detect changes in transmissibility. However, since our method is based on analytical estimates, analyses are fast and one can choose several time windows to analyse a dataset.

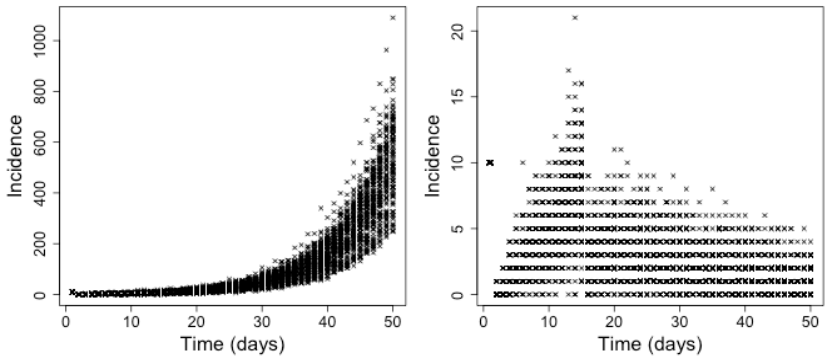

Web Figure 1 : Simulated epidemic curves in scenarios with constant instantaneous reproduction R=2.5 (left), constant R before (R=2.5) and after (R=0.7) a control measure on day 15 (right). 100 epidemics were simulated for each scenario, using a SARS-like serial interval.

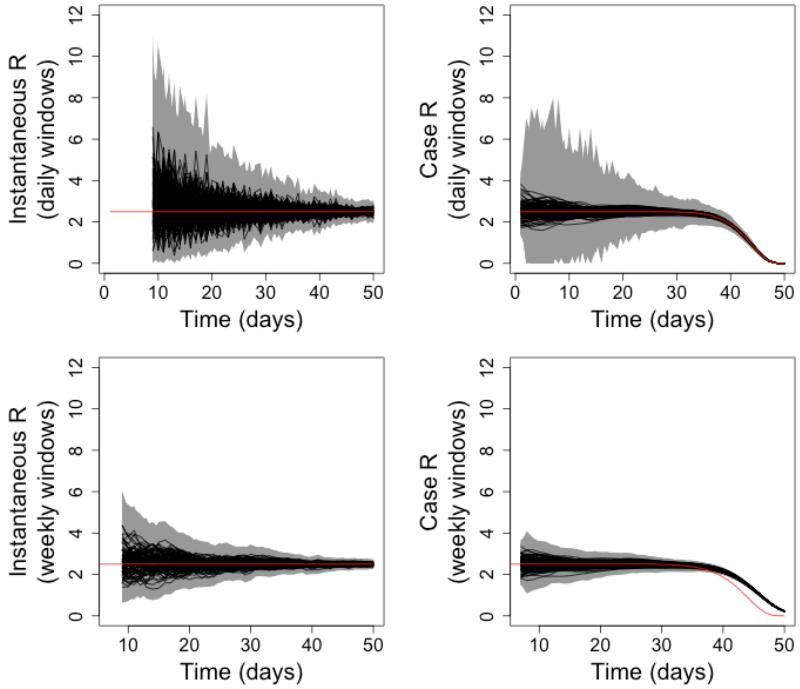

Web Figure 2 : Instantaneous reproduction number (left panels) and case reproduction numbers (right panels) estimated, for 100 epidemics simulated under scenario 1 (constant transmissibility) by our method and the Wallinga and Teunis (WT) method respectively, on daily windows (top panels) and sliding weekly windows (bottom panels). The black lines show the mean estimates and the grey zones show the 95% credible (our method) or confidence (WT method) intervals. The red lines show the instantaneous reproduction number used for simulation (left panels) and the corresponding case reproduction numbers (right panels) calculated as in (1).

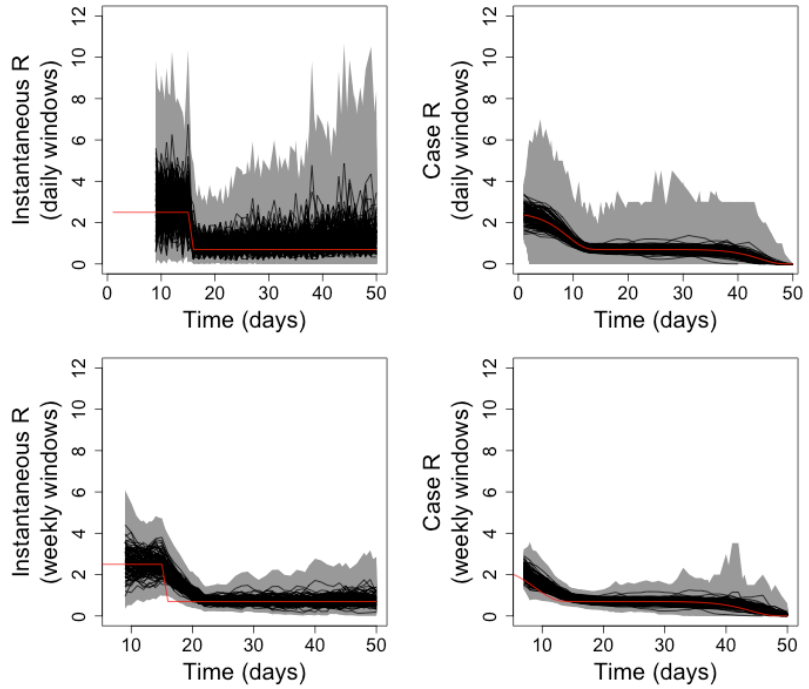

Web Figure 3 : Instantaneous reproduction number (left panels) and case reproduction numbers (right panels) estimated, for 100 epidemics simulated under scenario 2 (constant transmissibility before and after a control measure) by our method and the Wallinga and Teunis (WT) method respectively, on daily windows (top panels) and sliding weekly windows (bottom panels). The black lines show the mean estimates and the grey zones show the 95% credible (our method) or confidence (WT method) intervals. The red lines show the instantaneous reproduction number used for simulation (left panels) and the corresponding case reproduction numbers (right panels) calculated as in (1).

Web Appendix 7. Influence of incubation period distribution

In the previous section, we assumed that the incubation period was constant, so that in scenario 2 all cases infected just after the control measure would have symptoms on the same day. If the incubation period is not constant, the effect will be diluted and the changes in the instantaneous reproduction number estimated from the times series of symptoms onset will be less abrupt.

In this section, we present a simulation study designed to assess whether changes in transmissibility would still be detected if the incubation period was variable amongst individuals.

We considered the simulated epidemics presented in the previous section, but where the dates are the dates of infection rather than symptoms onset. The incubation period for each case was then drawn according to a discretized Gamma distribution with mean 3.81 days and variance 8.34 days^2 (4). The instantaneous and case reproduction numbers were then estimated from the times series of symptoms onset. Results are presented in Web Figures 4 and 5. Changes in transmissibility were still apparent in the estimates of the instantaneous reproduction number, but as expected, less clearly than in the scenario with constant incubation period. Generally speaking, the largest the variance in the incubation period, the lower the power to detect changes in transmissibility.

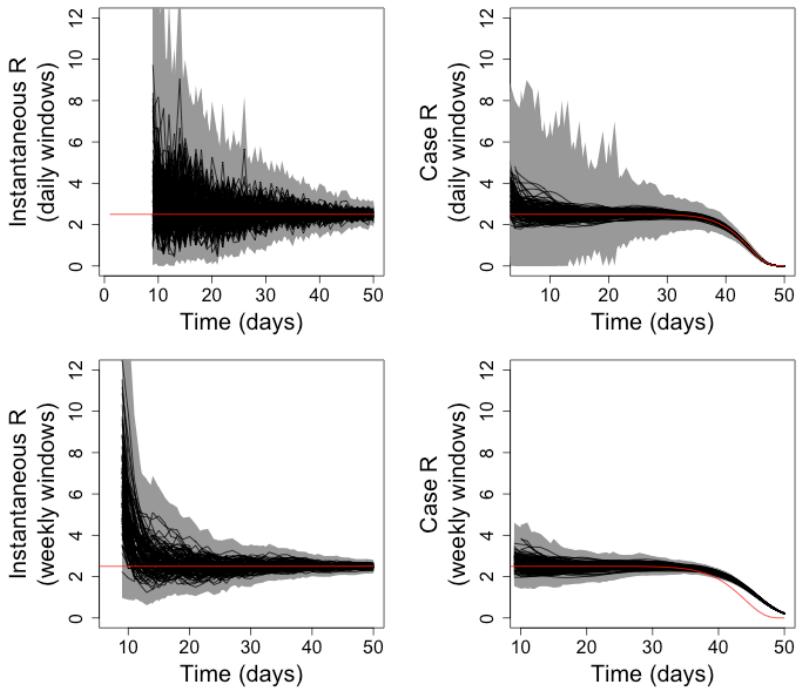

Web Figure 4 : Instantaneous reproduction number (left panels) and case reproduction numbers (right panels) estimated, for 100 epidemics simulated under scenario 1 (constant transmissibility) and assuming a non constant incubation period, by our method and the Wallinga and Teunis (WT) method respectively, on daily windows (top panels) and sliding weekly windows (bottom panels). The black lines show the mean estimates and the grey zones show the 95% credible (our method) or confidence (WT method) intervals. The red lines show the instantaneous reproduction number used for simulation (left panels) and the corresponding case reproduction numbers (right panels) calculated as in (1).

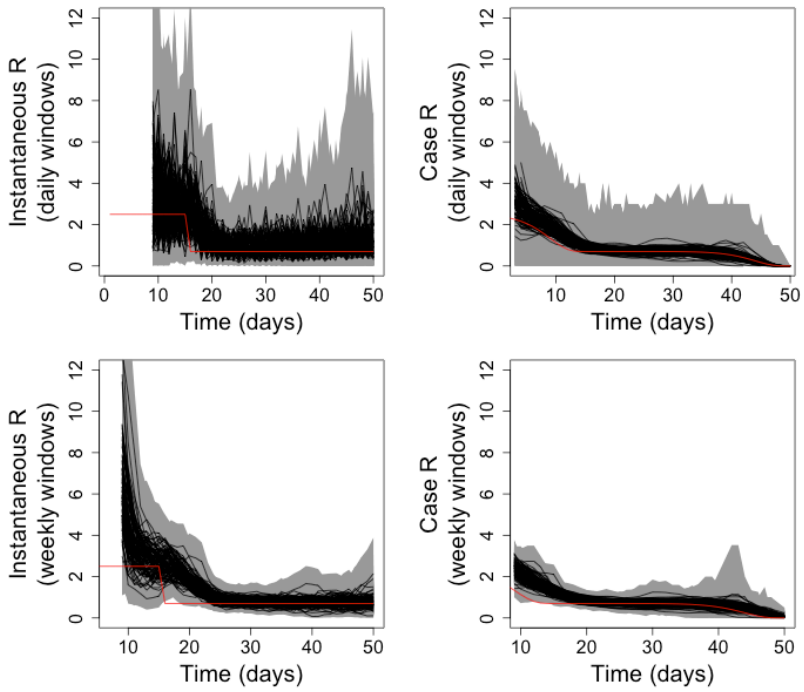

Web Figure 5 : Instantaneous reproduction number (left panels) and case reproduction numbers (right panels) estimated, for 100 epidemics simulated under scenario 2 (constant transmissibility before and after a control measure) and assuming a non constant incubation period, by our method and the Wallinga and Teunis (WT) method respectively, on daily windows (top

panels) and sliding weekly windows (bottom panels). The black lines show the mean estimates and the grey zones show the 95% credible (our method) or confidence (WT method) intervals. The red lines show the instantaneous reproduction number used for simulation (left panels) and the corresponding case reproduction numbers (right panels) calculated as in (1).

Web Appendix 8. Influence of underreporting

Simulations described in section 6 were further used to assess the influence of underreporting on the estimates of *R* obtained by using the time series of reported incidence. For each scenario, and for each of the 100 epidemics corresponding to that scenario, we simulated underreporting using a binomial distribution, with a constant reporting rate π varying between 20% and 100%. More precisely, for each day *t* of the epidemic, the number of reported cases O_t was drawn from a binomial distribution with parameters I_t (the true incidence on day t) and π. The instantaneous reproduction number was then reestimated crudely from O_t. The results are presented in Web Figures 6 and 7.

On average, the estimates of *R* from the reported cases only are similar to those obtained from all cases. However the credible intervals are wider for lower reporting rates (as expected since the number of cases in each time window is smaller, see section Web Appendix 2). Moreover, lower reporting rates lead to more variability in the mean estimates from one time window to the next, making it more difficult to detect changes in transmissibility.

Overall, underreporting does not appear to affect much the mean estimates of *R*, but affects the precision of those estimates.

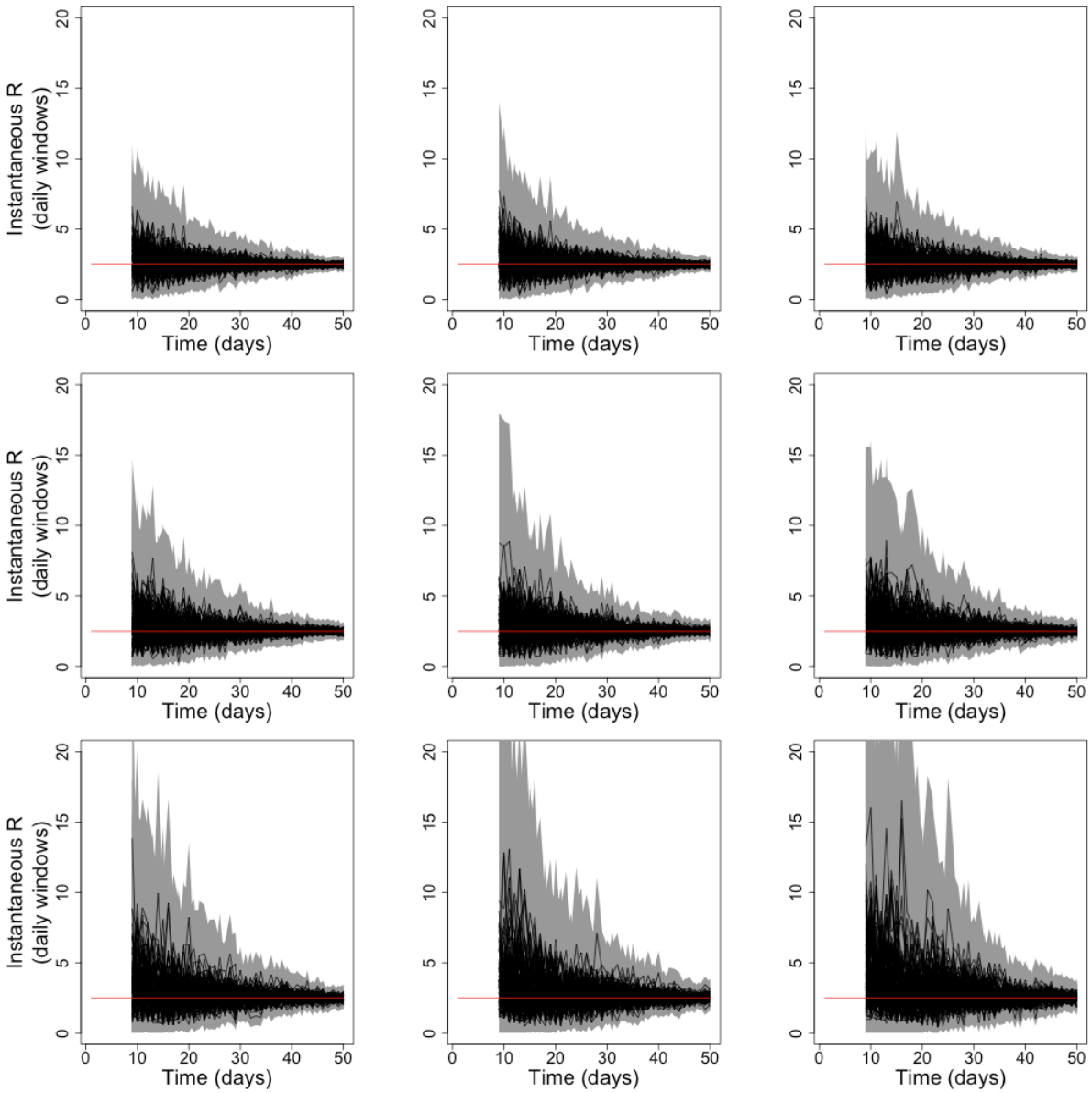

Web Figure 6 : Instantaneous reproduction number R estimated on daily windows for 100 epidemics simulated under scenario 1 (constant transmissibility), with varying reporting rates (100%, 90%, 80%, 70%, 60%, 50%, 40%, 30%, 20% respectively from top left to bottom right, line per line). The black lines show the mean estimates and the grey zones show the 95% credible intervals. The red lines show the R used for simulation.

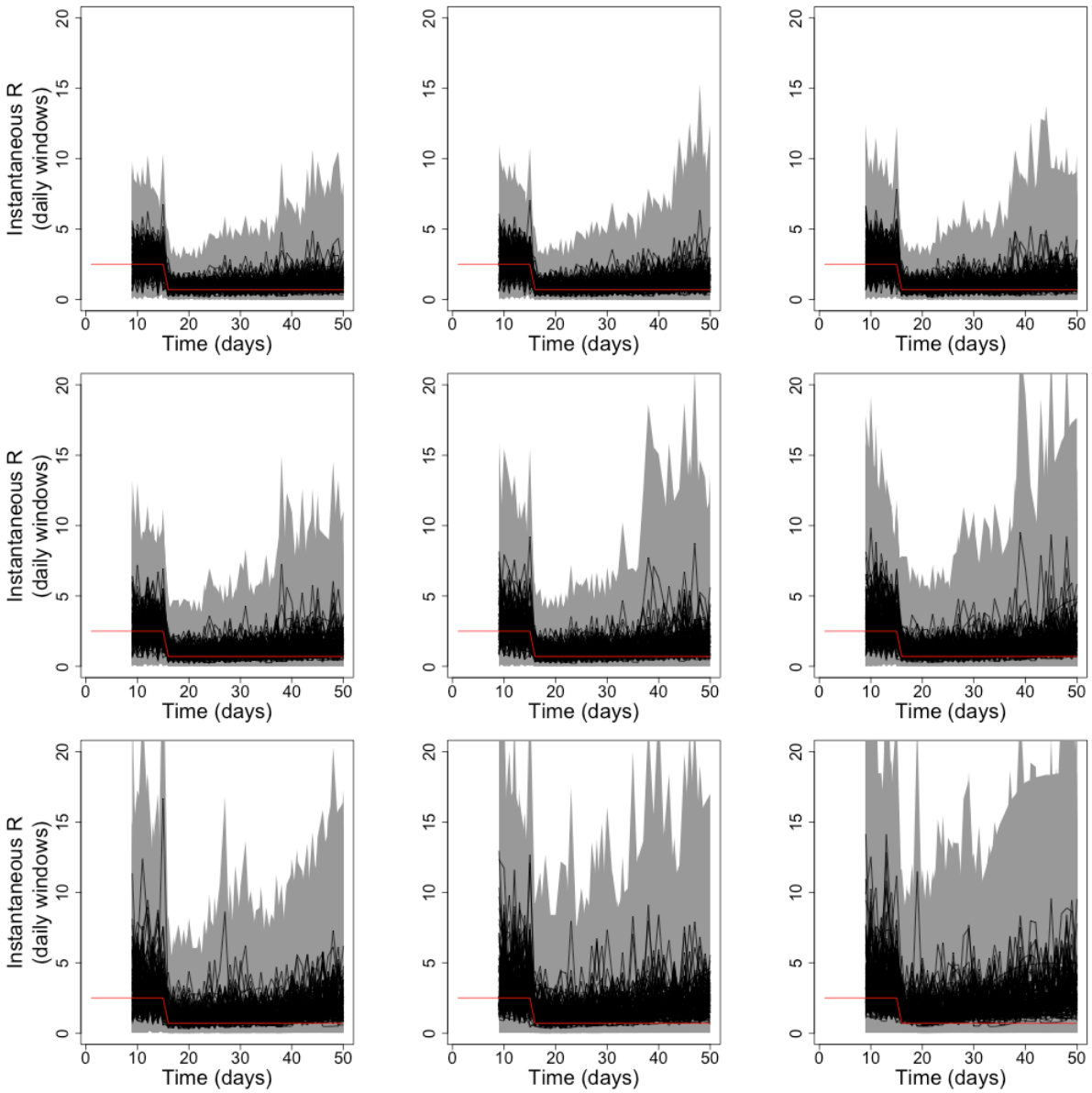

Web Figure 7: Instantaneous reproduction number R estimated on daily windows for 100 epidemics simulated under scenario 2 (constant transmissibility before and after a control measure), with varying reporting rates (100%, 90%, 80%, 70%, 60%, 50%, 40%, 30%, 20% respectively from top left to bottom right, line per line). The black lines show the mean estimates and the grey zones show the 95% credible intervals. The red lines show the R used for simulation.

Web Appendix 9. Using symptoms onset and serial interval leads to exact estimates for diseases where infectiousness follows symptoms onset

Our approach to estimate the reproduction number is developed for the ideal situation where times of infection are known and the infectivity profile w_s may be approximated by the distribution of the generation time (time from the infection of a primary case to infection of the cases he/she generates) (1). However, surveillance data typically report times of symptoms onset rather than times of infection,

and as a consequence the generation time distribution is difficult to ascertain, unlike the serial interval distribution.

In this section, we consider diseases for which infectiousness only starts at or after the time of symptom onset. We propose a model similar to that used in Ferguson et al. (5). Each infected individual *i* experiences an incubation period A_i during which he/she is not symptomatic and not infectious. The incubation period is independently identically distributed in all individuals according to a distribution φ. The incubation period ends at the time of symptoms onset, and from that time, individual *i* has an infectiousness profile given by a distribution ψ, independent on the incubation period in individual *i*. If *i* infects an individual *j*, the sequence of infection and symptoms onset in *i* and *j* can be represented as in Web Figure .

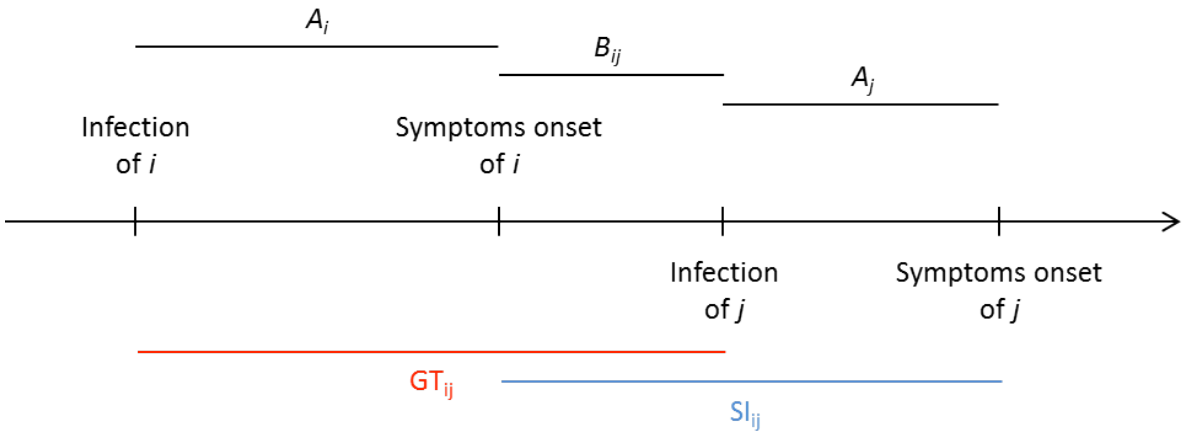

Web Figure 8: Generation time and serial interval

Note that in this model, B_{ij} is always positive as *i* is not infectious before symptoms onset. Moreover, the generation time and serial interval are given by $GT_{ij} = A_i + B_{ij}$ and $SI_{ij} = A_j + B_{ij}$ respectively. A_i, A_j and B_{ij} are independent, with respective distributions φ, φ and ψ. Hence the probability density functions of the generation time and the serial interval are given by $f_{GT} = \varphi * \psi$ and $f_{SI} = \varphi * \psi$ respectively, where $*$ is the convolution product, defined, for two probability density functions *f* and *g* by: $(f * g)(t) = \int_s f(t-s)g(s)ds$.

Therefore, in this case, the serial interval and the generation time have exactly the same distribution, and the estimates obtained using the serial interval distribution as the infectiousness profile will be exact. However, if the dates of symptoms onset are used instead of the dates of infection, the estimates are delayed, since R_t, estimated based on the new symptomatic individuals at time *t*, reflects in fact transmissibility at time $t - \delta$, where δ is the incubation period.

When the infectiousness profile ψ is not independent on the incubation period, the generation time and serial interval still have the same mean, but their variances can differ (6). To assess the extent to

which this could affect estimates of the instantaneous reproduction number obtained using the serial interval instead of the generation time, we reestimated *R* for the simulated epidemics described in section 6, but using a serial interval with standard deviation 2 times lower (respectively 2 times higher) than that used for the simulation (but same mean). Results are shown in Web Figure 9.

The instantaneous reproduction numbers reestimated with higher or lower standard deviation for the serial interval were able to capture changes in transmissibility. However, the mean estimates tended to be biased towards higher (respectively lower) values when a low (respectively high) standard deviation was used. In conclusion, using the serial interval distribution instead of the generation time distribution doesn't seem to affect the ability to detect changes in transmissibility, but overall, estimates of transmissibility might be slightly biased if the incubation period and the infectivity profile after symptoms are not independent.

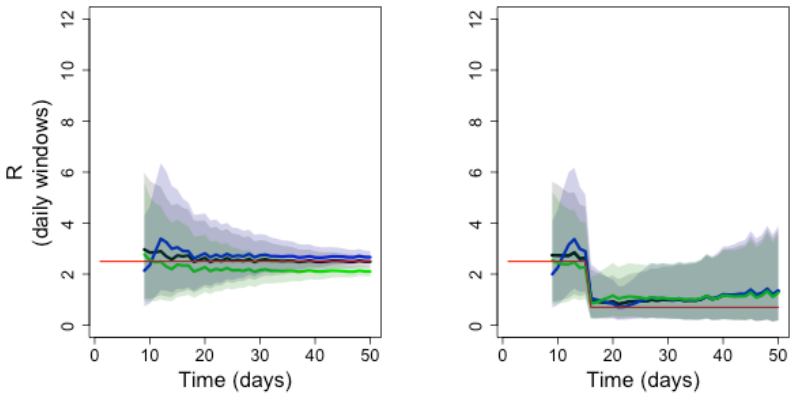

Web Figure 9: Instantaneous reproduction number (*R*) reestimated from 100 simulated datasets under one of two epidemic scenarios (left: constant transmissibility, right: constant transmissibility before and after a control measure) over daily windows. The red lines show the instantaneous reproduction numbers *R* used for simulation. The black lines show the average (over the 100 simulated epidemics) of the mean *R* reestimated using the serial interval distribution used for simulation; the grey shaded areas are delimited by the average lower and upper bounds of the 95% credible intervals estimated using the serial interval distribution used for simulation. The blue (respectively green) lines show the average of the mean *R* reestimated using a serial interval with standard deviation two time lower (respectively two times higher) than that used for simulation ; the blue (respectively green) shaded areas are delimited by the average lower and upper bounds of the 95% confidence intervals estimated using a serial interval with standard deviation two time lower (respectively two times higher) than that used for simulation .

Web Appendix 10. Influence of the prior on the mean and variance of the serial interval distribution

We took the example of the outbreak of pandemic flu in Baltimore in 1918 to assess how the choice of the prior distribution influences the estimates of R.

First, we assessed the influence of the prior mean and variance on the estimates of R. We explored four scenarios with respective prior means 1, 5, 10 and 50, and standard deviations equal to the means (hence CV=1). A pairwise comparison of the four scenarios showed that the median estimates and upper

and lower bounds of credible intervals for R differed by less than 5%, suggesting that the results were little sensitive to the choice of the prior mean and variance.

We also explored the impact on the estimates of R of changing the form of the prior distribution. To do so, we implemented a Monte Carlo Markov Chain (MCMC) procedure, with a simple Metropolis-Hastings algorithm to update the states of the Markov chain, to estimate *R* assuming a Weibull distributed prior. We compared the resulting *R* estimates with the analytical estimates obtained assuming a Gamma prior with same mean and standard deviation. The analysis was performed twice, with a prior mean of 1 and 5 respectively (and standard deviation equal to the mean). The estimates of *R* were very little sensitive to both the form of the prior distribution (Gamma or Weibull) and the mean prior (1 or 5), as shown in Web Figure 10.

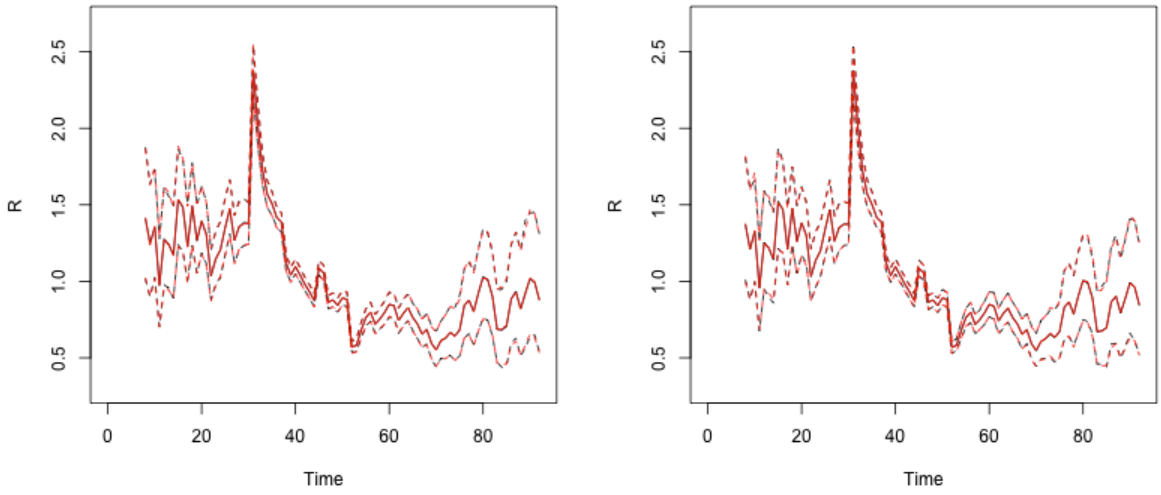

Web Figure 10: Daily estimates of the reproduction numbers *R* over sliding weekly windows for pandemic influenza in Baltimore, 1918, for a mean prior of 5 (left panel) and 1 (right panel); the black lines (hidden) correspond to Weibull prior and the red lines to Gamma prior; posterior medians are shown in plain line and 95% credible intervals in dotted lines.

Web Appendix 11. Discretization of serial interval distributions

Incidence data are typically discrete, so that the serial interval distribution needed to analyze them is discrete as well. However, most serial interval distributions, fitted to observations of transmission events in households for instance, are continuous. Here, we propose a formula to discretize the serial interval distribution.

We assume that the exact (i.e. continuous) time of infection of an incident case from day *t* is uniformly distributed on $\left[t;t+1\right[$. It can be shown that the delay *u* between the true times of infection of two cases that are incident on days *t* and *t+k* (*k≥0*) respectively is therefore distributed according to $f_U(u)=1_{k-1<u<k+1}\left[1-\left|u-k\right|\right]$.

To discretize the serial interval distribution, we weight its probability density function with the probability function of each delay:

$$w_k = \int_{k-1}^{k+1} f_{SI}(u) f_U(u)\,du$$

$$= (1+k)F_{SI}(k+1) - 2kF_{SI}(k) + (k-1)F_{SI}(k-1) + \int_{k-1}^{k} uf_{SI}(u)\,du - \int_{k}^{k+1} uf_{SI}(u)\,du$$

which sum to 1.

- **Shifted Gamma distribution**

Assuming the serial interval SI is such that $\mathrm{SI}-1$ is Gamma distributed with probability density function $\mathrm{f}_{\mathrm{SI}-1}(\mathrm{t})=\frac{1_{\mathrm{t}\geq 0}}{\Gamma(\mathrm{a})\mathrm{b}^{\mathrm{a}}}\mathrm{t}^{\mathrm{a}-1}\mathrm{e}^{-\frac{\mathrm{t}}{\mathrm{b}}}$, we find:

$$w_k = k * F_{\Gamma,a,b}(k) + (k-2) * F_{\Gamma,a,b}(k-2) - 2*(k-1) * F_{\Gamma,a,b}(k-1) + ab\left(2F_{\Gamma,a+1,b}(k-1) - F_{\Gamma,a+1,b}(k-2) - F_{\Gamma,a+1,b}(k)\right)$$

Where $F_{\Gamma,a,b}$ is the cumulative density function of a Gamma distribution with parameters (a,b).

This is the parameterization that was used for all analyses in the paper unless otherwise specified, and it is the parameterization implemented in both the Excel® (Microsoft Excel®, Redmond, WA) tool and the *R* package.

- **Shifted Weibull distribution**

Assuming the serial interval SI is such that $\mathrm{SI}-1$ is Weibull distributed with probability density function $\mathrm{f}_{\mathrm{SI}-1}(\mathrm{t})=1_{\mathrm{t}\geq 0}\frac{\mathrm{a}}{\mathrm{b}}\left(\frac{\mathrm{t}}{\mathrm{b}}\right)^{\mathrm{a}-1}\mathrm{e}^{-\left(\frac{\mathrm{t}}{\mathrm{b}}\right)^{\mathrm{a}}}$, we find:

$$w_k = k * F_{W,a,b}(k) + (k-2) * F_{W,a,b}(k-2) - 2*(k-1) * F_{W,a,b}(k-1) + ke^{-\left(\frac{k}{b}\right)^a} + (k-2)e^{-\left(\frac{k-2}{b}\right)^a} - 2(k-1)e^{-\left(\frac{k-1}{b}\right)^a} - \frac{b}{a}\left[\gamma\left(\frac{1}{a},\left(\frac{k}{b}\right)^a\right) + \gamma\left(\frac{1}{a},\left(\frac{k-2}{b}\right)^a\right) - 2*\gamma\left(\frac{1}{a},\left(\frac{k-1}{b}\right)^a\right)\right]$$

where $F_{W,a,b}$ is the cumulative density function of a Weibull distribution with parameters (a,b), and $\gamma(s,x)=1_{x>0}\int_0^x t^{s-1}e^{-t}dt$ is the incomplete Gamma function.

Web Appendix 12. Influence of the shape of the serial interval distribution

We took the example of the outbreak of pandemic flu in Baltimore in 1918 to assess how the shape of the serial interval distribution influences the estimates of R.

We explored three distributions for the serial interval:

- a discretized Gamma distribution with mean 2.6 days and standard deviation 1.5 day
- a discretized Weibull distribution with same mean and variance
- a manually constructed discrete distribution with same mean and variance but a different form.

Despite differences in the shape of the serial interval (especially between the manually constructed one and the two other ones), the estimates of *R* were very similar in all three scenarios, as shown in Web Figure 11.

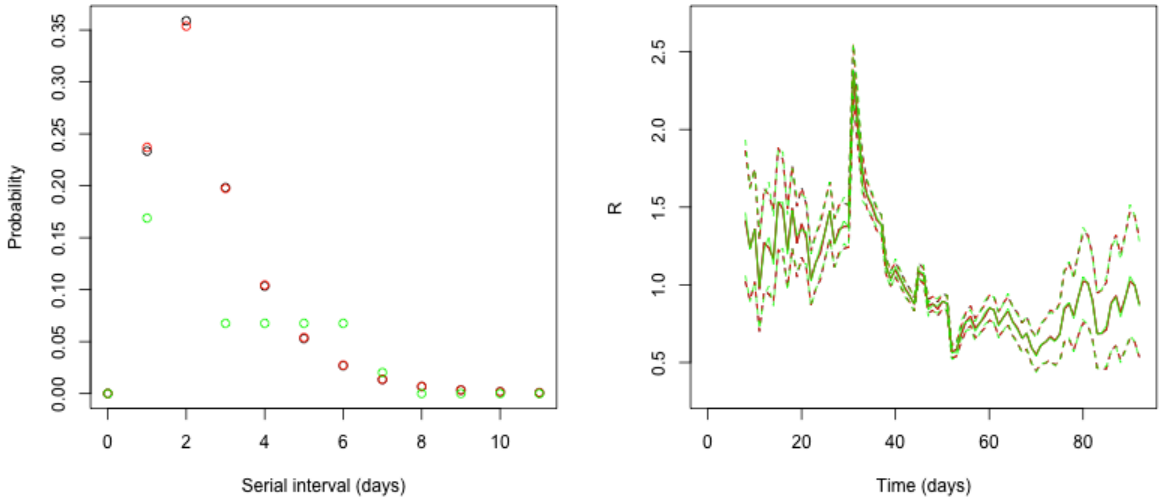

Web Figure 11: Influence of the serial interval shape on the estimates of the reproduction number. Gamma (black), Weibull (red) and manually constructed (green) serial interval distributions with common mean and variance (left panel). Daily estimates of the reproduction numbers *R* over sliding weekly windows for pandemic influenza in Baltimore, 1918, using these three serial interval distributions (right panel); posterior medians are shown in plain line and 95% credible intervals in dotted lines.

Web Appendix 13. Derivation of the serial interval distribution for Measles and Smallpox

For all the outbreaks analysed in this article, we assumed a Gamma distribution for the serial interval, with mean and standard deviation taken from the literature. However, for measles and smallpox, the mean and standard deviation of the serial interval were not available directly from previous studies. They were derived indirectly from articles which reported related quantities such as the latency and the infectious period. In this section, we explain how to derive the serial interval distribution in a model with latency L and infectious period I. First we consider a model with constant infectiousness over the infectious period, and then we consider a model in which the infectious period is split in two periods with two different levels of infectiousness.

13.1. Measles: classical model with constant infectiousness over infectious period

Svensson (6) shows that in such a model, the probability density function (pdf) of the serial interval (SI) is $f_{GT}(x) = \left[f_L * \left(\frac{1-F_I}{\mathbf{E}[I]} \right) \right](x)$, where f_L is the pdf of the latency period L, F_I is the cumulative density function (CDF) of the infectious period I, $\mathbf{E}[I]$ is the average infectious period, and $*$ stands for the convolution operator.

The mean serial interval is therefore $\mathbf{E}[GT] = \mathbf{E}[L] + \frac{1}{\mathbf{E}[I]} \int_{x=0}^{+\infty} \left(1 - F_I(x)\right) x dx = \mathbf{E}[L] + \frac{\mathbf{E}[I^2]}{2\mathbf{E}[I]}$, and its variance is $\mathbf{Var}[GT] = \mathbf{Var}[L] + \frac{1}{\mathbf{E}[I]} \int_{x=0}^{+\infty} \left(1 - F_I(x)\right) x^2 dx - \left(\frac{\mathbf{E}[I^2]}{2\mathbf{E}[I]}\right)^2$. In the case where I is Gamma distributed with parameters (a_I, b_I) ($\mathbf{E}[I] = a_I b_I$ and $\mathbf{Var}[I] = a_I b_I^2$), the variance of the serial interval is therefore equal to:

$$\mathbf{Var}[GT] = b_I{}^2 \left(\frac{1}{12} a_I{}^2 + \frac{1}{2} a_I + \frac{5}{12} \right) + \mathbf{Var}[L]$$

In order to estimate the mean and variance of the serial interval for measles, we used these formulae together with the estimates of the average latency period (10.3 days) and of the standard deviation of the latency period (2.6 days) and the assumptions on the infectious period (leading to an average infectious period of 8.9 days and a standard deviation of 1.7 days) found in Groendyke et al. (7).

13.2. Smallpox: model with infectious period split in two parts with constant infectiousness over each part

We now consider a model in which the infectious period is split in two successive periods F and R, with two different levels of infectiousness. We assume that infectiousness during the second part (R) is k times infectivity during the first part (F).

A similar reasoning than for the model with constant infectiousness shows that the pdf of the serial interval is: $f_{GT}(x) = \left[f_L * \left(\frac{(1 - F_F) + k f_F * (1 - F_R)}{\mathbf{E}[F] + k\mathbf{E}[R]} \right) \right](x)$, where f_L is the pdf of the latency period L, F_F and F_R are the CDF of the first and second parts of the infectious period respectively, $\mathbf{E}[F]$ and $\mathbf{E}[R]$ are the corresponding means, and * stands for the convolution operator.

After simplification, the mean serial interval is $\mathbf{E}[GT] = \mathbf{E}[L] + \frac{\mathbf{E}[F^2] + k\mathbf{E}[R^2] + 2k\mathbf{E}[R]\mathbf{E}[F]}{2\left(\mathbf{E}[F] + k\mathbf{E}[R]\right)}$

and its variance is:

$$\mathbf{Var}[GT] = \mathbf{Var}[L] - \left(\frac{\mathbf{E}[F^2] + k\mathbf{E}[R^2] + 2k\mathbf{E}[R]\mathbf{E}[F]}{2\left(\mathbf{E}[F] + k\mathbf{E}[R]\right)} \right)^2 + \frac{1}{3\left(\mathbf{E}[F] + k\mathbf{E}[R]\right)} \int_{t=0}^{+\infty} f_F(t) t^3 dt + \frac{k}{3\left(\mathbf{E}[F] + k\mathbf{E}[R]\right)} \left[\int_{u=0}^{+\infty} f_R(u) u^3 du + 3\mathbf{E}[R^2]\mathbf{E}[F] + 3\mathbf{E}[R]\mathbf{E}[F^2] \right]$$

In the case where F and R are Gamma distributed, the variance becomes

$$\mathbf{Var}[GT] = \mathbf{Var}[L] - \left(\frac{a_F b_F{}^2 (1+a_F) + k a_R b_R{}^2 (1+a_R) + 2k a_R b_R a_F b_F}{2(a_F b_F + k a_R b_R)} \right)^2 + \frac{b_F{}^3 (a_F+2)(a_F+1)a_F + k b_R{}^3 (a_R+2)(a_R+1)a_R + 3k a_R b_R a_F b_F \left[(1+a_R) b_R + (1+a_F) b_F \right]}{3(a_F b_F + k a_R b_R)}$$

In order to estimate the mean and variance of the serial interval for smallpox, we used these formulae together with the estimated durations of the latency (mean 11.6 days, variance 3.36 days^2), fever (mean 2.49 days, variance 0.89 days^2)and rash (mean 16.0 days, variance 18.3 days^2) periods, and the estimated relative infectiousness during the rash period compared to the fever period ($k = 6.4$) found in Riley and Ferguson (8).

Web Appendix 14. Guide for using the Excel® tool

In this section, we provide step-by-step guidance to using our Excel® tool to estimate instantaneous reproduction numbers from a time series of incidence and a serial interval distribution.

1. Open the Excel® file Estimation_R_instantaneous.xls

There are several sheets in it : Readme, Data, Output1 serial interval, Output2 R estimates and Figures. Readme will provide you with information on how to use the document, which is summarized in this document.

Data is the only sheet which needs to be modified; only light coloured cells have to be modified.

2. Fill in the Incidence section as shown in Snapshot 1.

Snapshot 1: Filling in the incidence section

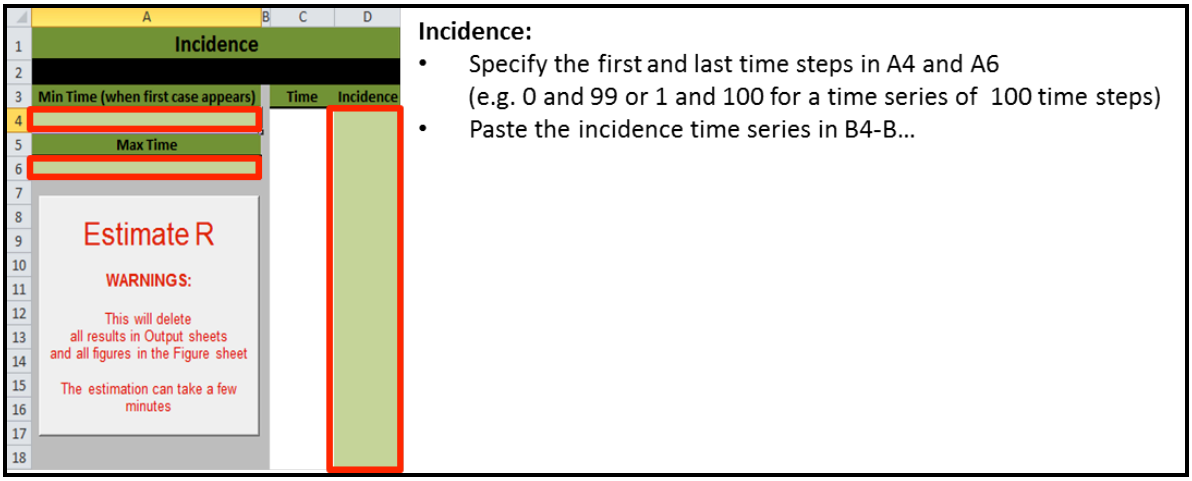

3. Specify your assumptions about the serial interval distribution (see snapshot 2).

Snapshot 2: Specifying the serial interval distribution

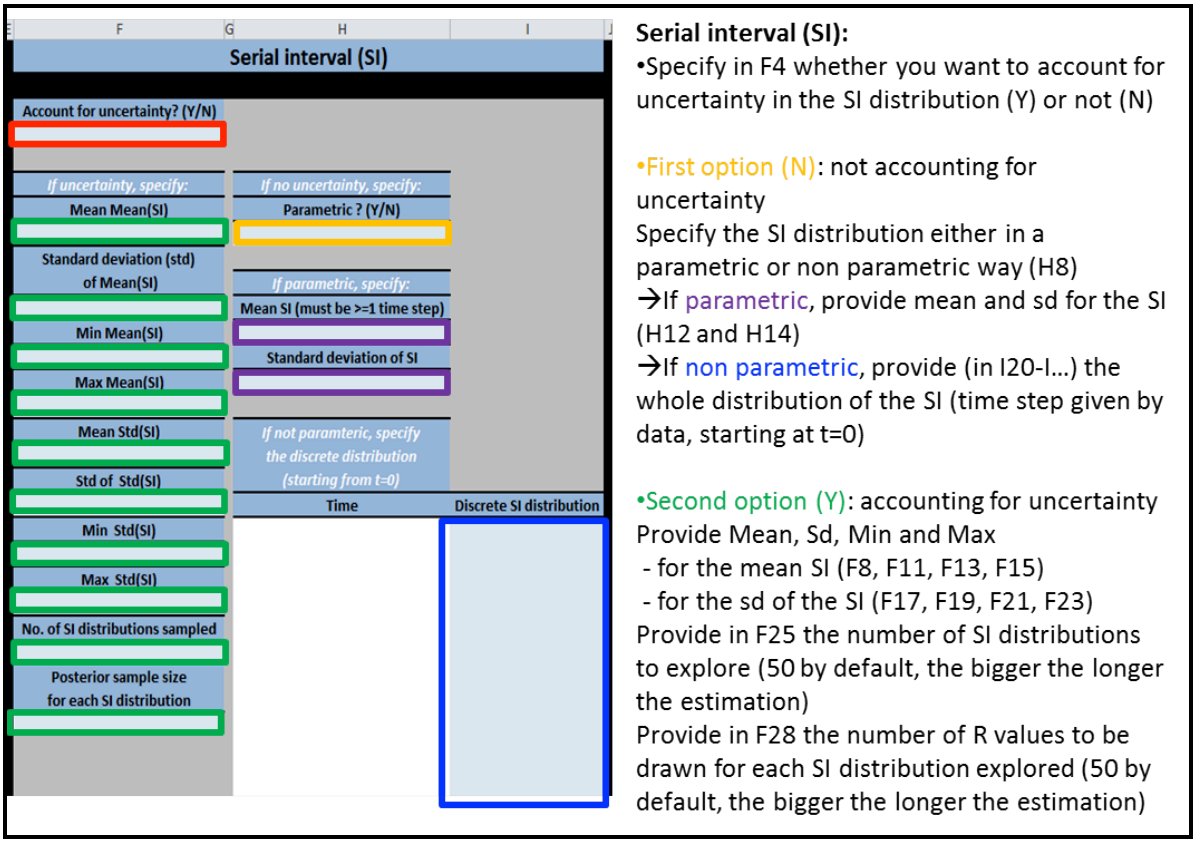

4. Specify the time windows you want to use (see snapshot 3). Keep the posterior coefficient of variation to its default value of 0.3

Snapshot 3: Choosing the time windows for estimation of R

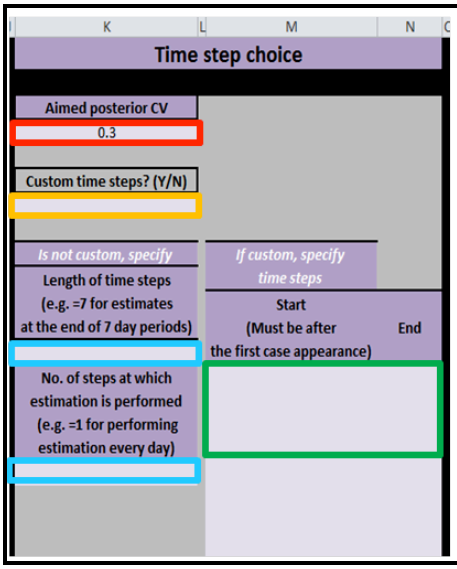

Time windows:

•Specify in K4 the aimed posterior coefficient of variation (default 0.3, the smaller the more precise the R estimates but the longer the time windows need to be to get this precision)

•Specify in K7 whether you will use custom time windows (Y) or not (N)

•First option (N): custom time windows

Give start times in M14-M… and end times in N14-N…

Time windows can overlap.

•Second option (Y): non custom time windows

Give the length of windows in K13 (eg 7 if daily data and weekly widows)

Give, in K18, the number of time windows at which estimation is performed (1 suggested to get estimates on sliding windows ending on each time step with data)

5. Specify the prior mean and standard deviation (see snapshot 4).

Snapshot 4: Specification of the prior distribution

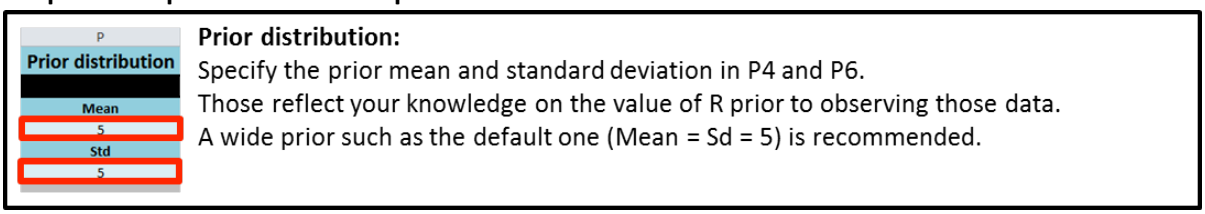

6. Enable Macros

Macros need to be enabled in order to run the estimation of R. Refer to the documentation of Excel® specific to the version you are using to know how to enable the macros.

7. Run the estimation

Snapshot 5: Running the estimation

8. Reading the results

Results are presented as tables in sheets “Output1 serial interval” and “Output2 R estimates” and as figures in sheet “Figures”.

References

1. Fraser C. Estimating individual and household reproduction numbers in an emerging epidemic. PLoS ONE 2007;2(1):e758.
2. Wallinga J, Teunis P. Different epidemic curves for severe acute respiratory syndrome reveal similar impacts of control measures. Am J Epidemiol 2004;160(6):509-16.
3. Cauchemez S, Boelle PY, Thomas G, Valleron AJ. Estimating in real time the efficacy of measures to control emerging communicable diseases. Am J Epidemiol 2006;164(6):591-7.
4. Donnelly CA, Ghani AC, Leung GM, Hedley AJ, Fraser C, Riley S, et al. Epidemiological determinants of spread of causal agent of severe acute respiratory syndrome in Hong Kong. Lancet 2003;361(9371):1761-6.
5. Ferguson NM, Cummings DA, Cauchemez S, Fraser C, Riley S, Meeyai A, et al. Strategies for containing an emerging influenza pandemic in Southeast Asia. Nature 2005;437(7056):209-14.
6. Svensson A. A note on generation times in epidemic models. Math Biosci 2007;208(1):300-11.
7. Groendyke C, Welch D, Hunter DR. Bayesian Inference for Contact Networks Given Epidemic Data. Scandinavian Journal of Statistics 2011;38(3):600-616.
8. Riley S, Ferguson NM. Smallpox transmission and control: spatial dynamics in Great Britain. Proc Natl Acad Sci U S A 2006;103(33):12637-42.